Lithos 294–295 (2017) 97–111

Contents lists available at ScienceDirect

Lithos

journal homepage: www.elsevier.com/locate/lithos

# Age and geochemistry of the intrusive rocks from the Shaquanzi-Hongyuan Pb–Zn mineral district: Implications for the Late Carboniferous tectonic setting and Pb–Zn mineralization in the Eastern Tianshan, NW China

Wan-Jian Lu [a,b], Hua-Yong Chen [a,c,*], Li Zhang [a], Jin-Sheng Han [a], Bing Xiao [a], Deng-Feng Li [d], Wei-Feng Zhang [e], Cheng-Ming Wang [a,b], Lian-Dang Zhao [a,b], Hong-Jun Jiang [a]

[a] Key Laboratory of Mineralogy and Metallogeny, Guangzhou Institute of Geochemistry, Chinese Academy of Sciences, Guangzhou 510640, China
[b] Graduate University of Chinese Academy of Sciences, Beijing 100049, China
[c] Guangdong Provincial Key Laboratory of Mineral Physics and Materials, 511 Kehua Street, Guangzhou 510640, China
[d] School of Marine Sciences, Sun Yat-sen University, Guangzhou 510006, China
[e] Wuhan Institute of Geology and Mineral Resources, China Geological Survey, Wuhan 434205, China

ARTICLE INFO

*Article history:*
Received 17 March 2017
Accepted 10 October 2017
Available online 13 October 2017

*Keywords:*
Eastern Tianshan
Shaquanzi-Hongyuan Pb–Zn deposits
Geochemistry
Late Carboniferous

ABSTRACT

The Central Tianshan Terrane (CTT) in the Eastern Tianshan (Xinjiang, NW China) is an important Pb–Zn metallogenic belt and played a pivotal role in crustal evolution and collisional tectonics of the southern Central Asian Orogenic Belt. The Shaquanzi gabbro and Hongyuan granodiorite are located in the northern margin of the CTT and associated with Pb–Zn mineralization. Zircon U–Pb dating yielded weighted mean ages of 307.2 ± 1.5 Ma and 301.2 ± 1.5 Ma for the Shaquanzi gabbro and the Hongyuan granodiorite, respectively. These rocks are medium-K calc-alkaline series and enriched in large ion lithophile elements (LILEs; e.g., K, Rb, Ba) and depleted in high field strength elements (HFSEs; e.g., Nb, Ta, Ti), displaying typical arc affinities.

The Shaquanzi gabbro shows low Nb/Ta (11.0–14.2), a high $Mg^{\#}$ range (56–59), positive zircon $\varepsilon_{Hf}(t)$ (+3.30 − +7.26) and whole rock $\varepsilon_{Nd}(t)$ (+0.70 − +1.38) values, and low $I_{Sr}$ ratios (0.704858–0.705137), which indicate that the protolith was probably derived from the sub-continental lithospheric mantle that had been metasomatized by subduction-related fluids. The Hongyuan granodiorite contains hornblende but lack of Al-rich minerals and has low $I_{Sr}$ ratios (0.704769–0.706211 < 0.707), suggesting an I-type origin. Moreover, the Hongyuan granodiorite has positive $\varepsilon_{Hf}(t)$ (+1.12 − +5.57) and $\varepsilon_{Nd}(t)$ (+0.38 − +1.86) values, with high $Mg^{\#}$ (52), variable Nb/Ta ratios (12.6–12.9), low contents of Ni, Cr and Co and Pb isotopes ($^{206}Pb/^{204}Pb$ = 17.461–18.299, $^{207}Pb/^{204}Pb$ = 15.541–15.581, $^{208}Pb/^{204}Pb$ = 37.456–38.129), suggesting the Hongyuan granodiorite was generated by partial melting of juvenile crust sources mixed with some mantle-derived materials.

Combined published works with our new geochronological, geological, geochemical and isotopic data, we propose that the CTT may have evolved from a continental arc to a syn-collisional setting during the period of ca. 307–301 Ma. The continuing southward subduction of the Junggar oceanic slab beneath the CTT in the Late Carboniferous resulted in extensive arc-related volcanic rocks emplacement that had indirect links to the Pb–Zn mineralization (e.g., reworked/upgraded).



## 1. Introduction

Located between the European and Siberia Cratons to the north and the Tarim and North China cratons to the south (Fig. 1A), the Central Asian Orogenic Belt (CAOB) has experienced a long-lived evolution of multiple accretion of continents, microcontinents, arc systems and accretionary complexes in the Paleo-Asian Ocean (Jahn et al., 2000; Sengör et al., 1993; Sengör and Natal'in, 1996; Windley et al., 2007; Zhang et al., 2016a, 2016b, 2016c, 2017; Xiao et al., 2012, 2015).

The Junggar Ocean, situated between the Junggar terrane to the north and the Central Tianshan Terrane (CTT) and Yili block to the south (Fig. 1B), represents a major southern segment of the Paleo-Asian Ocean, making its subduction and closure crucial to the understanding of the accretionary and collisional processes of the southern

* Corresponding author at: Key Laboratory of Mineralogy and Metallogeny, Guangzhou Institute of Geochemistry, Chinese Academy of Sciences, Guangzhou 510640, China.
*E-mail address:* huayongchen@gig.ac.cn (H.-Y. Chen).

https://doi.org/10.1016/j.lithos.2017.10.009
0024-4937/

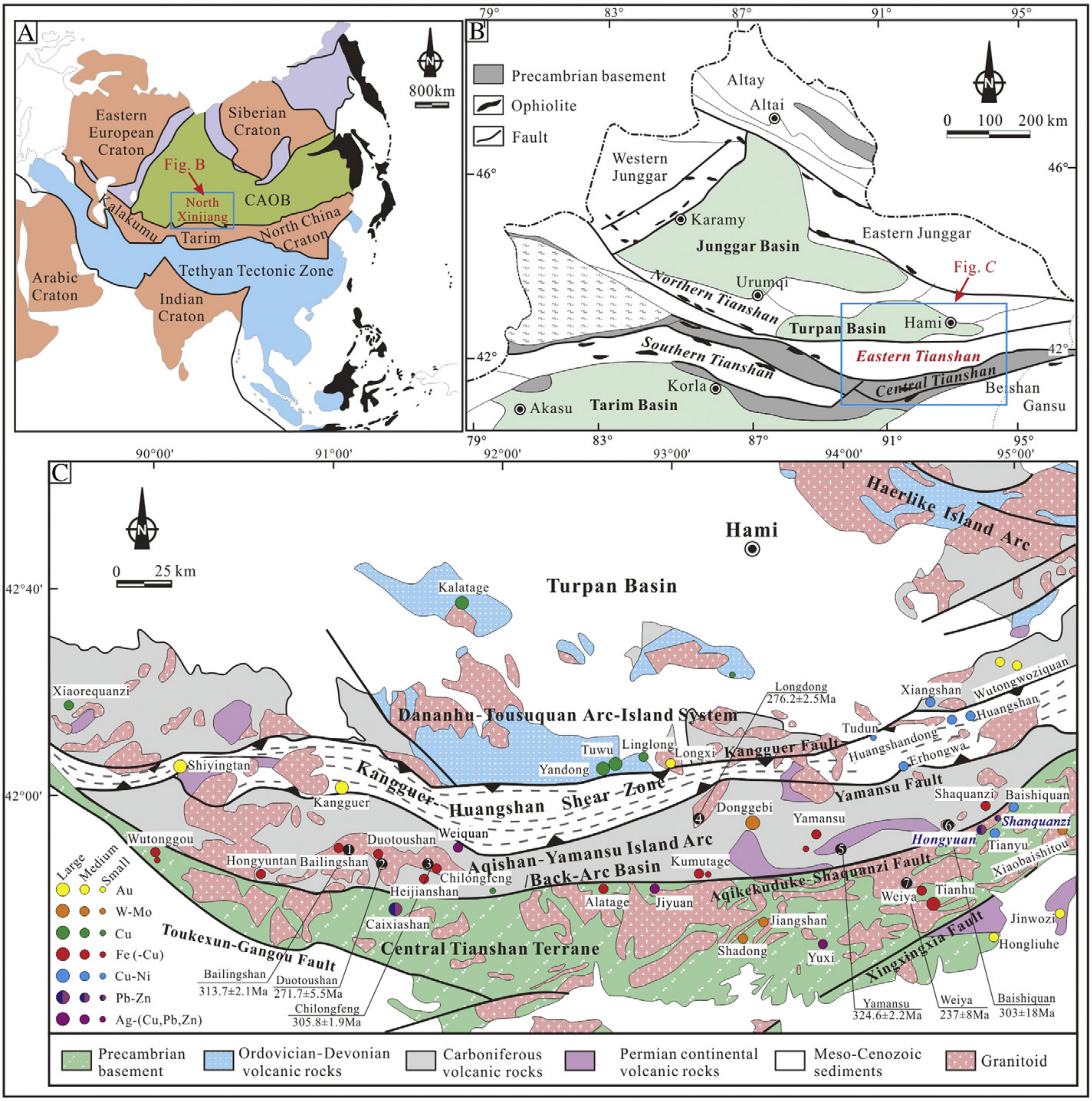


**Fig. 1.** (A) Simplified geological map of the Central Asian Orogenic Belt (CAOB; modified after Sengör and Natal'in, 1996), (B) Sketch map showing the tectonic framework of North Xinjiang (after Xiao et al., 2008; Y.J. Chen et al., 2012) and (C) Geologic map of the Eastern Tianshan Orogenic Belt, showing the distribution of major ore deposits (modified after Deng et al., 2014; Wang et al., 2006). Chronological data from: W.F. Zhang et al. (2016), Zhang et al. (2005), Zhang et al. (2015b), Zhao et al. (2017) and Zhou et al. (2010).

CAOB (Windley et al., 1990; Xiao et al., 2012, 2015). However, the timing of its closure is still hotly debated, with suggestions ranging from the Early Carboniferous (Gao et al., 1998), through the Late Carboniferous–Early Permian (Charvet et al., 2007; Chen et al., 2011; Zhang et al., 2015a, 2015, 2016a), to the Permian–Triassic (W.J. Xiao et al., 2009), leading to various competing models proposed for the Paleozoic evolution of the Eastern Tianshan (an important component of the southern CAOB).

The oldest basement rocks in the Eastern Tianshan occur in the CTT, which is one of the most important Pb–Zn metallogenic provinces in northwestern China, including the giant Caixiashan, Hongyuan, Shaquanzi, Hongxingshan, Jiyuan and Yuxi Pb–Zn (–Ag) deposits (Fig. 1C). Previous studies indicated that the Pb–Zn ore-hosting Precambrian basement had undergone various degrees of reworking by the Carboniferous magmatism (Cao et al., 2013; Gao et al., 2007; H.Y. Chen et al., 2012; Lu et al., 2017; Peng et al., 2006, 2007; Q.H. Xiao et al., 2009; Zhong et al., 2008; Zhou et al., 1999). However, the geodynamic setting and genesis of these Pb–Zn deposits and their associated igneous rocks remains unclear.

Representative intrusive rocks were collected from the Shaquanzi and Hongyuan Pb–Zn deposits (located in the CTT), including gabbro and granodiorite, which reworked the Shaquanzi and Hongyuan Pb–Zn orebodies, respectively (Lu et al., 2017; Zhong et al., 2008). In this study, we report whole-rock geochemical and zircon U–Pb and Lu–Hf isotope data from Shaquanzi and Hongyuan. We then discuss the petrogenesis of these intrusive rocks and the Late Carboniferous tectonic implications for the Eastern Tianshan.

## 2. Geology background

### 2.1. Regional geology

The Chinese Tianshan Orogen is bordered between the Tarim Craton to the south and the Junggar terranes to the north (Fig. 1A, B) (Allen et al., 1993; Charvet et al., 2007; Gao et al., 1998; Windley et al., 1990; Xiao et al., 2012), which can be geographically divided into the western and eastern segments roughly along 86°E longitude (Charvet et al., 2007; Gao et al., 2009; Zhang et al., 2016a, 2017; Xiao et al., 2004). This study mainly focuses on the Eastern Tianshan, which can be tectonically subdivided into the North Tianshan (NTS), Central Tianshan Terrane (CTT) and South Tianshan (STS), separated from each other by major strike-slip faults (Charvet et al., 2007; Zhang et al., 2016a, 2017; Xiao et al., 2004). The tectonic framework of the Eastern Tianshan was primarily influenced by the development of two sub-oceans of the Paleo-Asian Ocean, namely (a) the Junggar Ocean between the CTT and Junggar terranes and (b) the South Tianshan Ocean between the CTT and Tarim Craton (Ma et al., 1997; Windley et al., 1990; Zhang et al., 2016a, 2017; Xiao et al., 2004).

The NTS accretionary belt is composed dominantly of a series of Devonian–Carboniferous island arcs (Fig. 1B, e.g., Bogda, Dananhu, Yamansu) and Carboniferous–Jurassic imbricated strata, genetically controlled by the subduction and closure of the Junggar Ocean (e.g., Han et al., 2010; Ma et al., 1997). A primarily southward subduction of the Junggar Ocean beneath the Chinese Tianshan has been substantiated by not only detailed kinematic investigations in the region (Charvet et al., 2007; Laurent-Charvet et al., 2002; Shu et al., 1999) but also the findings of Late Ordovician (ca. 450 Ma) thickened lower curst-derived adakitic rocks (Zhang et al., 2016b), high-pressure basic-intermediate granulites (Shu et al., 2004) and Early Paleozoic to Late Carboniferous subduction-related magmatic rocks (e.g., Ma et al., 2014; Shi et al., 2014; Zhang et al., 2015b, 2016a) along the northern margin of the CTT.

As the most essential portion of the Chinese Tianshan, the CTT comprises mainly of Precambrian basement with minor Paleozoic volcanosedimentary formations (Hu et al., 2000; Lei et al., 2011; Li et al., 2007; Liu et al., 2004; Shu et al., 2004; Xiao et al., 2004) and a number of granitoids (Fig. 1C). The basement is consisted of the Mesoproterozoic Xingxingxia and Kawabulag Groups and the Neoproterozoic Tianhu Group, and has been metamorphosed to upper greenschist- to amphibolite-facies (Gao et al., 1993; Luo, 1989). The Xingxingxia Group represents the oldest rocks in the CTT, and comprises mainly amphibolite- to granulite-facies marble, schist, gneiss and migmatite (He et al., 2014; Hu et al., 1986, 2000). The Late Mesoproterozoic Kawabulake Group is composed of meta-carbonatite, schist and granitic gneiss (He et al., 2014; Xiu et al., 2002). The Tianhu Group distributed between the Jianshanzi and Hongliuhe areas comprises mainly schist, quartzite, marble and minor amphibolite, with protoliths of terrigenous clastics intercalated with minor mafic volcanics (Liu et al., 2004).

The STS accretionary belt, characterized by widespread ophiolitic mélanges and a well-studied Carboniferous high-pressure/low-temperature (HP/LT) metamorphic belt (Gao et al., 1998; Gao and Klemd, 2003; Long et al., 2006; Wang et al., 2011), is believed to have been formed by the closure of the South Tianshan Ocean between the CTT and the northern Tarim Craton (Gao and Klemd, 2003; Huang et al., 2015; Wang et al., 2011).

### 2.2. Deposit geology

#### 2.2.1. Shaquanzi Pb–Zn deposit

The Shaquanzi Pb–Zn deposit is situated at ~170 km southeast of the city of Hami in Xinjiang, NW China (Fig. 1C), and ~4 km south of the Shaquanzi Fault. The exposed strata are the Kawabulake Group silicified marble, marble, banded carbonaceous marble and minor dolomitic marble. Quaternary sediments, situated southwest of Shaquanzi, are dominated by alluvial gravel, sand and clay.

The gabbro presented in the northern part of the Shaquanzi deposit. In the vicinity of the Shaquanzi Pb–Zn deposit, the contact metamorphism generated some calc–silicate skarn. Mafic and felsic dykes and quartz veins are extensively exposed in the district (Fig. 2).

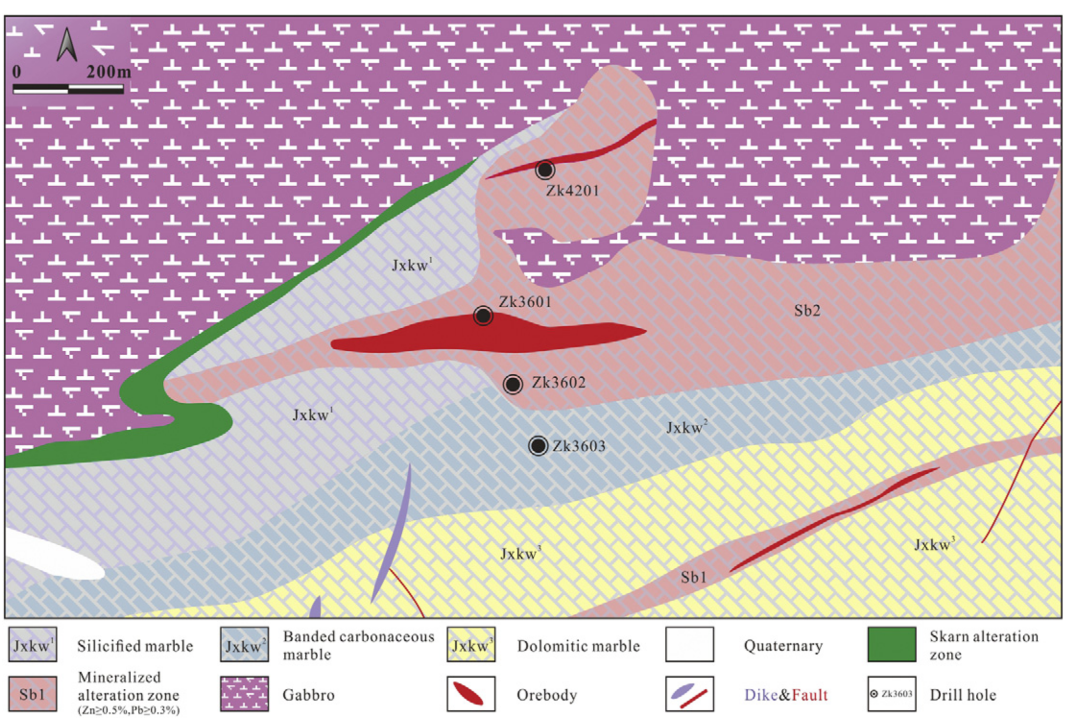


**Fig. 2.** Deposit geology of the Shaquanzi Pb–Zn deposit (modified after Xinjiang BGMR).

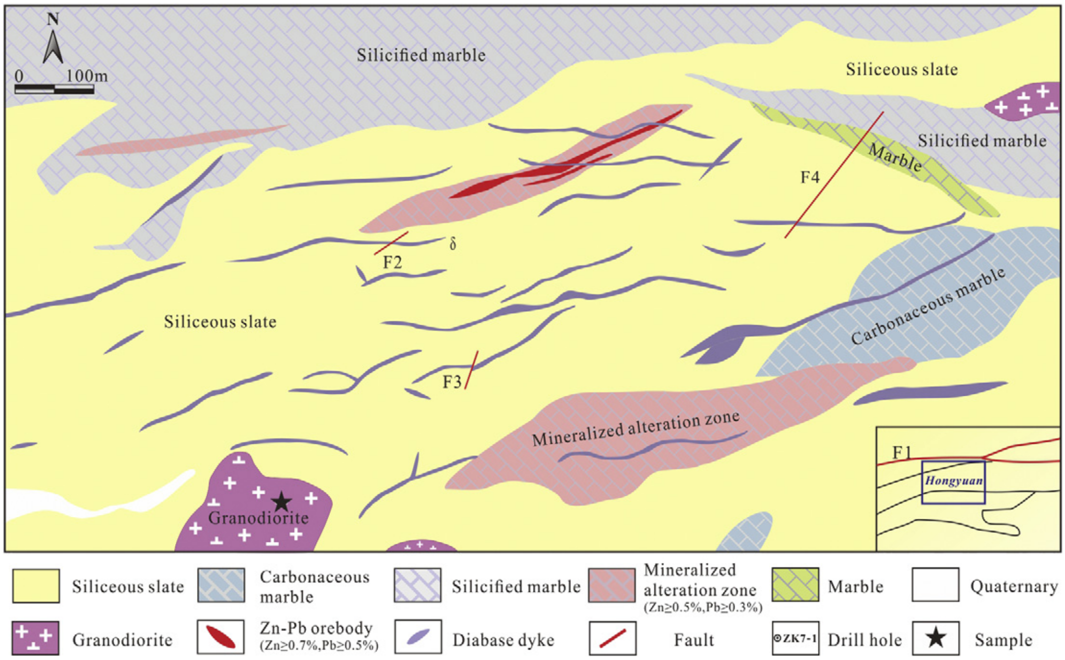


**Fig. 3.** Deposit geology of the Hongyuan Pb–Zn deposit (modified after Lu et al., 2017).

Nine stratabound orebodies (200–300 m long and 0.7–10.4 m thick) have been delineated at Shaquanzi (Zhong et al., 2008). The major orebodies are hosted by carbonaceous marble and generally have limonite, tremolite and actinolite alterations. Ore minerals include fine- to medium-grained sphalerite and galena accompanied by abundant pyrite and pyrrhotite.

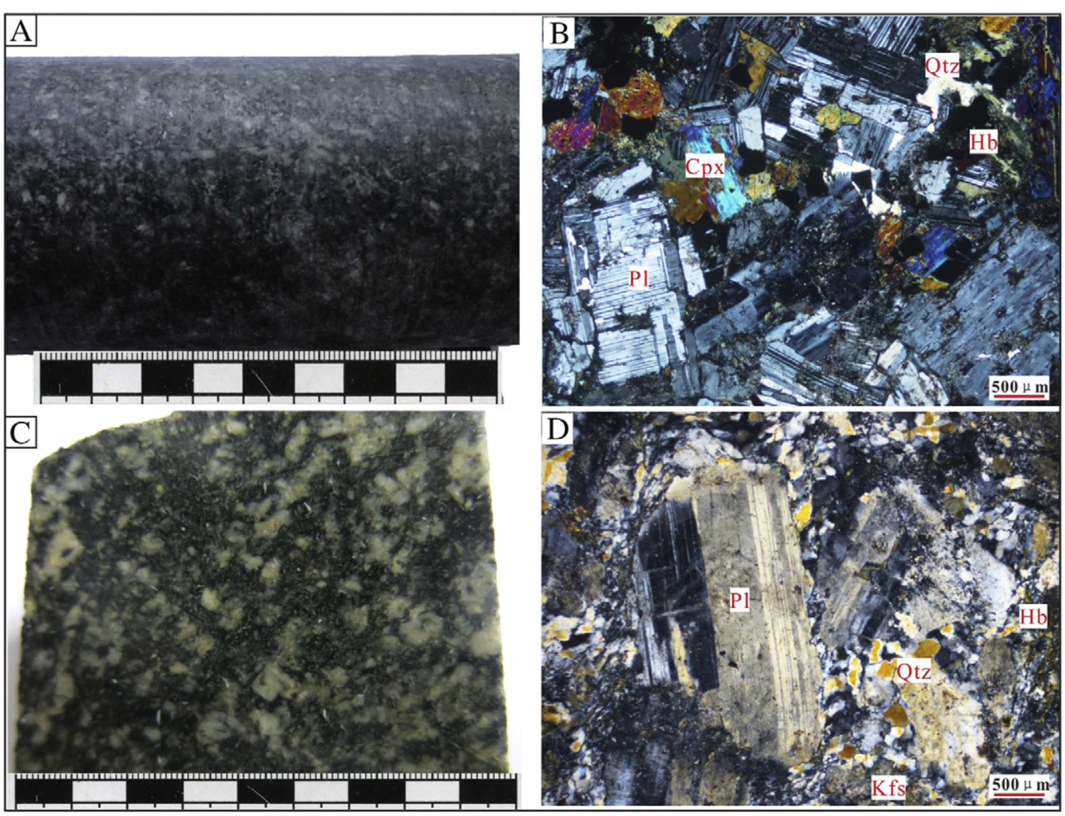


**Fig. 4.** Hand specimen and thin sections of the Shaquanzi and Hongyuan intrusive rocks. (A–B) Shaquanzi gabbro; (C–D) Hongyuan granodiorite. Abbreviations: Pl = plagioclase; Qtz = quartz; Hb = hornblende, Kfs = K-feldspar; Cpx = clinopyroxene.

*2.2.2. Hongyuan Pb–Zn deposit*

The Hongyuan Pb–Zn deposit (~5 km southwest of Shaquanzi) (Fig. 1C) is located to the south and tectonically controlled by the Shaquanzi Fault. Outcropping strata at Hongyuan are the Mesoproterozoic Kawabulake Group carbonaceous marble and siliceous slate. Late Paleozoic intrusions (dominantly Carboniferous granodiorite) are mainly distributed in the northern and southern parts of Hongyuan (Fig. 3).

The major Hongyuan orebodies are hosted by siliceous slate and carbonaceous marble, commonly epidote and diopside altered. Thirteen EW-trending stratabound orebodies (ca. 50–500 m long and tens of meters thick) (Fig. 3) were delineated. Major metallic minerals include fine- to medium-grained sphalerite and galena, which are accompanied by abundant pyrite, pyrrhotite and minor chalcopyrite. Alteration types at Hongyuan include mainly silicic, carbonate, diopside, tremolite and chlorite alterations (Lu et al., 2017).

## 3. Sampling and analytical methods

*3.1. Sampling*

Following detailed geological sampling, three least altered gabbro samples from Shaquanzi (drill hole Zk4201; Fig. 2) and three granodiorite samples from Hongyuan (Fig. 3) were collected.

The Shaquanzi gabbro (*SZ1–30*; Fig. 4A, B) and the Hongyuan granodiorite (*HY-N*; Fig. 4C, D) intruded the Mesoproterozoic Kawabulake Group. The dark-grayish gabbro displays fine- to medium-grained hypidiomorphic texture, and is composed mainly of subhedral tabular plagioclase (40–45 vol%), clinopyroxene (10–20 vol%), irregularly-shaped hornblende (20–25 vol%) and quartz (15–25 vol%). Some plagioclase grains are potassic and argillic altered. The granodiorite is a dark-grayish and medium- to coarse-grained, and contains plagioclase (40–56 vol%), quartz (15–25 vol%), K-feldspar (10–20 vol%), hornblende (3–8 vol%) and biotite (2–5 vol%). Some hornblende grains are slightly chlorite altered.

*3.2. Analytical methods*

Whole-rock major element analyses were performed at the ALS Chemex Company in Guangzhou (Guangzhou, China), analyzed by X-ray fluorescence spectrometry (XRF) for major elements, with the analysis precision better than $\pm 2\%$. Trace element concentrations were measured at the State Key Laboratory of Ore Deposit Geochemistry, Guiyang Institute of Geochemistry (Guiyang, China), with analytical uncertainties generally $<5\%$. Zircons were separated from Shaquanzi gabbro (*SZ1–30*) and Hongyuan granodiorite (*HY-N*) samples, using standard density and separation magnetic techniques. Then, the selected zircons were conducted for cathodoluminescence (CL) imaging, U–Pb dating and in situ Lu–Hf isotope analyses at the Guangzhou Institute of Geochemistry (Guangzhou, China). Whole-rock Sr–Nd–Pb isotope analysis was performed using a Micromass Isoprobe MC-ICP-MS at the State Key Laboratory of Isotope Geochemistry, Guangzhou Institute of Geochemistry (Guangzhou, China). Detailed analytical procedures are given in online Appendix A.

## 4. Results

*4.1. Whole-rock major and trace elements*

Whole-rock major and trace element compositions of the Shaquanzi and Hongyuan rocks are listed in Table A.1.

The Shaquanzi gabbro samples contain $SiO_2$ = 48.5–49.5 wt%, $Al_2O_3$ = 16.0–18.3 wt%, CaO = 8.6–9.1 wt%, $K_2O$ = 0.9–1.1 wt%, $Na_2O$ = 2.7–2.9 wt%, with $Na_2O/K_2O$ ratios of 2.4–3.1. Their $Fe_2O_3^T$ and MgO contents range 9.6–10.4 wt% and 5.2–6.3 wt%, respectively, corresponding to the $Mg^{\#}$ values of 56–59. Three gabbro samples fall inside the gabbro field in the $SiO_2$ vs. Nb/Y diagram (Fig. 5A), similar with the Late Carboniferous mafic rocks from the CTT (Zhang et al., 2016a). The gabbro rocks generally show medium-K calc-alkaline

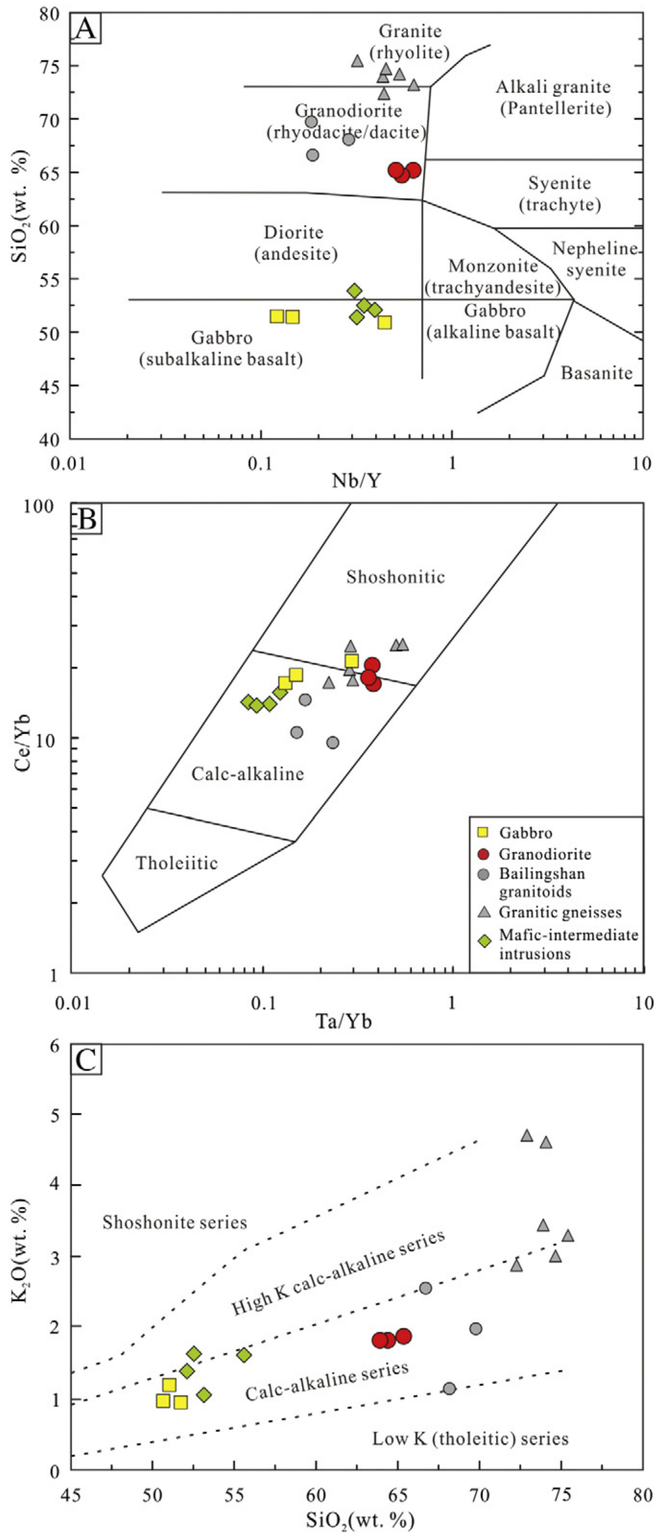


**Fig. 5.** (A) $SiO_2$ vs. Nb/Y diagram (modified after Winchester and Floyd, 1977), (B) Ce/Yb vs. Ta/Yb diagram (after Müller et al., 1992) and (C) $K_2O$ vs. $SiO_2$ diagram (after Peccerillo and Taylor, 1976) for the Shaquanzi and Hongyuan intrusive rocks. Late Carboniferous Bailingshan granitoids, granitic gneisses and mafic–intermediate intrusions data are from W.F. Zhang et al. (2016), Zhang et al., 2015b, 2016a).

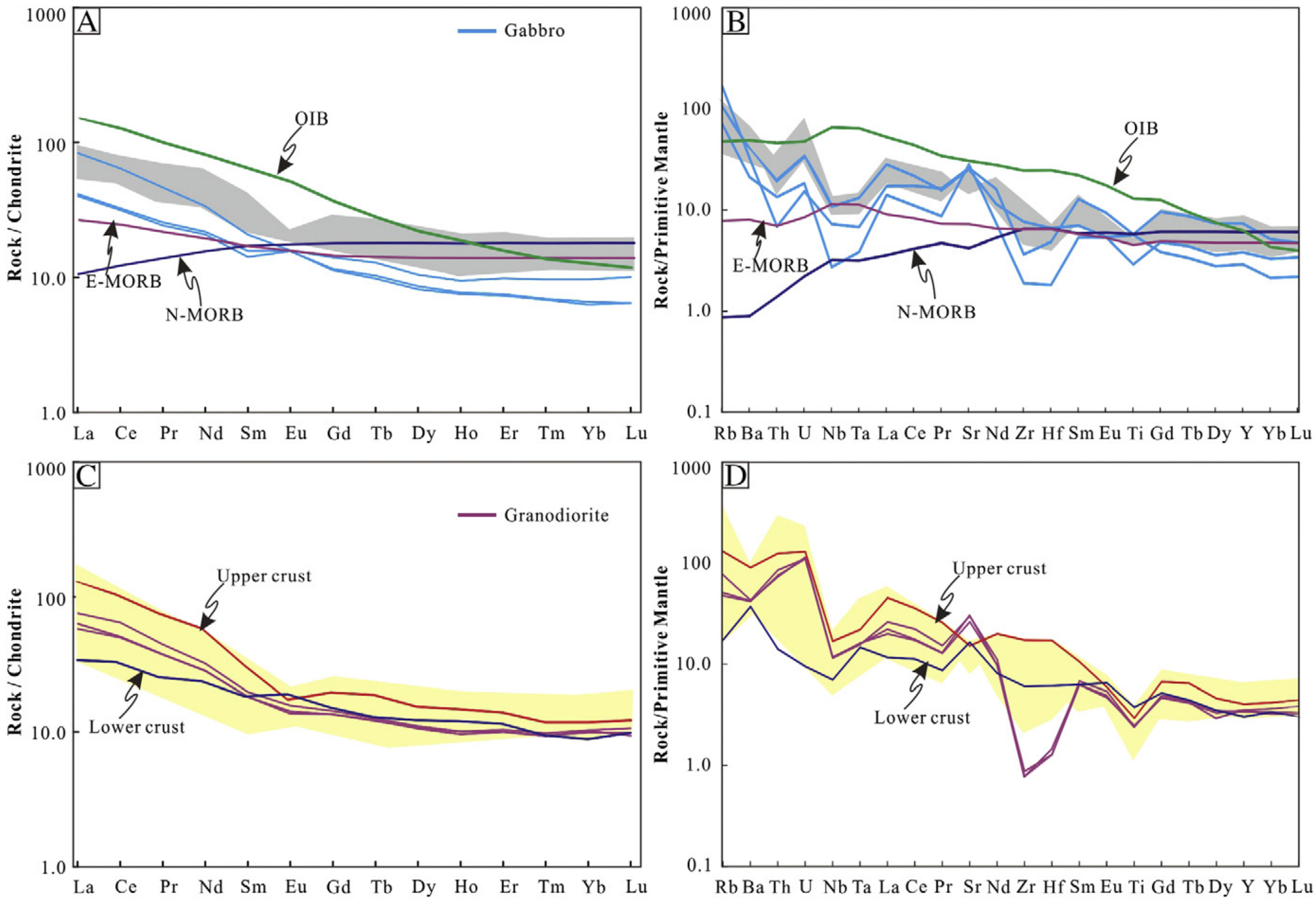


**Fig. 6.** Chondrite-normalized REE patterns and Primitive mantle-normalized multi-element diagrams for the representative samples. (A–B) Shaquanzi gabbro; (C–D) Hongyuan granodiorite. The gray shaded areas denote the Late Carboniferous CTT mafic–intermediate intrusions (W.F. Zhang et al., 2016) and the yellow shaded areas denote the Late Carboniferous granites from CTT and Bailingshan (W.F. Zhang et al., 2016; Zhang et al., 2015b). Data of the average chondrite, primitive mantle, E-MORB, N-MORB and OIB are from Sun and McDonough (1989). Data of the upper and lower crust are from Rudnick and Gao (2003).

affinities (Fig. 5) and have low total REE contents (52–94 ppm), exhibiting slightly right-inclined REE patterns ($(La/Yb)_N = 6.06$–8.61, $(Tb/Yb)_N = 1.34$–1.57, $\delta Eu = 0.93$–1.22; Fig. 6A). In the primitive-mantle normalized trace element diagram, the gabbro samples show enrichments in large ion lithophile elements (LILEs; e.g., Rb, Ba and Sr)) and depletions in high field strength elements (HFSEs; e.g., Nb, Ta and Ti) (Fig. 6B).

The Hongyuan granodiorite samples contain $SiO_2$ (62.7–63.0 wt%), $Al_2O_3$ (16.3 wt%) and CaO (4.3–5.1 wt%), lower $TiO_2$ (0.5 wt%), $K_2O$ (1.7–1.8 wt%) and $Na_2O$ (3.8–3.9 wt%), with $Na_2O/K_2O$ ratios of 2.2. With $Fe_2O_3^T$ (4.8–4.9 wt%) and MgO (2.2–2.3 wt%), the three granodiorite samples have average $Mg^{\#}$ values of 52, belonging to medium-K calc-alkaline series (Fig. 5). The rocks have total REE contents of 75–91 ppm, and display right-inclined REE patterns ($(La/Yb)_N = 5.62$–7.64, $(Tb/Yb)_N = 1.17$–1.27, $\delta Eu = 0.87$–0.93 (Fig. 6C). In the primitive-mantle normalized trace element diagram, the granodiorite samples show enrichments in large-ion lithophile elements (LILEs; e.g., Rb and Sr) and strong depletions in high field strength elements (HFSEs; e.g., Nb, Ta and Ti) (Fig. 6D).

*4.2. Zircon U–Pb ages and Lu–Hf isotopic compositions*

Representative CL images, U–Pb ages and $\varepsilon_{Hf}(t)$ values of the analyzed zircons are shown in Fig. A.1. Most zircon grains are euhedral to subhedral, transparent to semi-transparent and light brown or colorless, with lengths of 50 to 100 μm and aspect ratios between 1:1 and 4:1. Most crystals show well-developed oscillatory zoning in CL images, together with their relatively high Th/U ratios (0.41–1.02; Table A.2), suggesting an igneous origin (Rubatto, 2002), consistent with the HREE enrichment, positive Ce anomalies and negative Eu anomalies (Fig. 7B, D; Table A.3) in zircon REE patterns (Hoskin and Schaltegger, 2003; Rubatto, 2002).

Twenty zircons from the Shaquanzi gabbro (*SZ1–30*) yielded $^{206}Pb/^{238}U$ ages of 311–302 Ma and a weighted mean age of 307.2 ± 1.5 Ma (1σ; MSWD = 0.67), which can be used to represent the formation age of the Shaquanzi gabbro (Fig. 7A; Table A.2). Thirty-one analyses were undertaken on zircons from the Hongyuan granodiorite (*HY-N*). Excluding one old inherited zircon (332 Ma), the remaining 30 zircons yielded $^{206}Pb/^{238}U$ ages of 307–295 Ma and a weighted mean age of 301.2 ± 1.5 Ma (1σ; MSWD = 0.53) that can be considered as the formation age for the Hongyuan granodiorite (Fig. 7C; Table A.2).

Results of the Lu–Hf isotope analysis are given in Table A.4 and shown in Fig. 8. Twelve zircons from the Shaquanzi gabbro yielded $^{176}Hf/^{177}Hf$ ratios of 0.282683 to 0.282795, corresponding to $\varepsilon_{Hf}(t)$ values of +3.30 to +7.26 and $T_{DM2}$ model ages of 1107–855 Ma (Table A.4). Eleven zircons from the Hongyuan granodiorite yielded initial $^{176}Hf/^{177}Hf$ ratios of 0.282302 to 0.282745, corresponding to $\varepsilon_{Hf}(t)$ values of −10.26 to +5.57 and $T_{DM2}$ model ages of 1965–966 Ma (Table A.4).

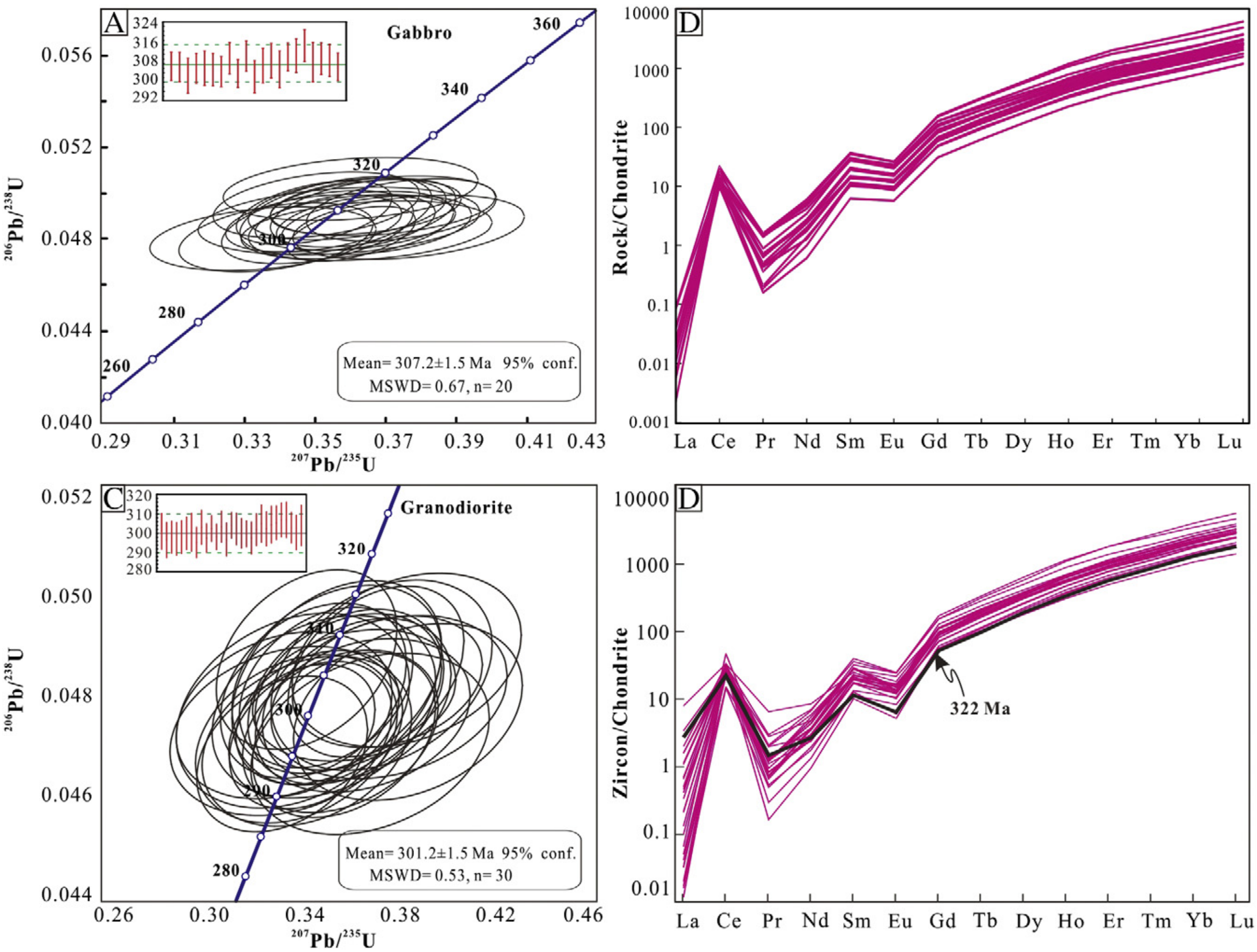


**Fig. 7.** Zircon U–Pb concordia diagram and weighted mean $^{206}Pb/^{238}U$ ages and chondrite-normalized REE patterns of zircon grains from the representative samples. (A–B) Shaquanzi gabbro; (C–D) Hongyuan granodiorite. Data of the average chondrite are from Sun and McDonough (1989).

### 4.3. Whole-rock Sr–Nd–Pb isotopes

Whole-rock Sr, Nd and Pb isotope compositions of the Shaquanzi and Hongyuan rocks are listed in Table A.5 and shown in Fig. 9. Initial isotopic ratios were calculated back to the crystallization ages of the studied rocks.

The gabbro samples show $I_{Sr}$ ratios of 0.704858–0.705137, $\varepsilon_{Nd}(t)$ values of $+0.70 - +1.38$ and $T_{DM}$ model ages of 1.22–1.04 Ga. The

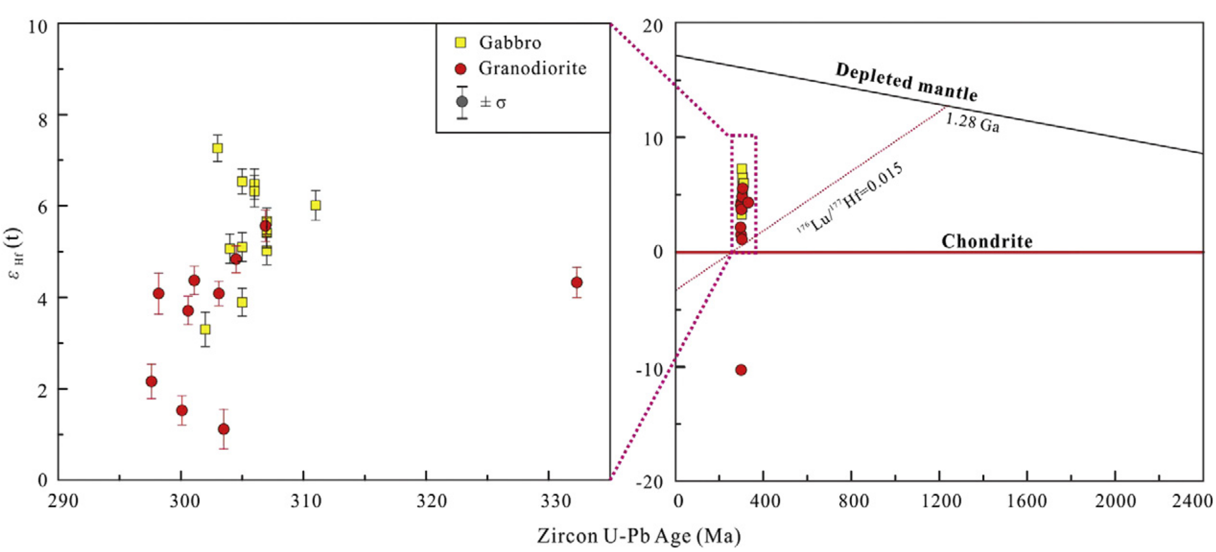


**Fig. 8.** Zircon Hf isotopes for the Shaquanzi and Hongyuan intrusive rocks.

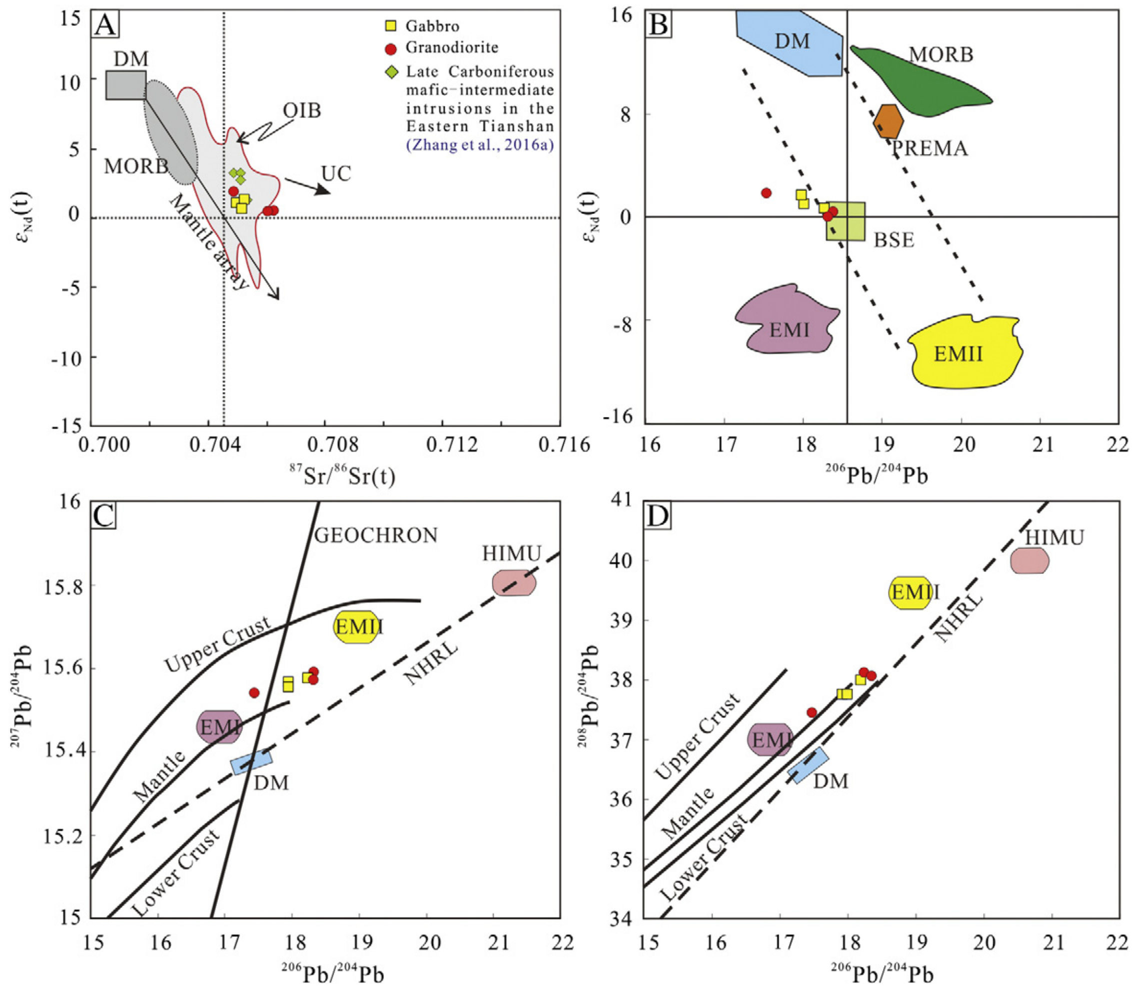


**Fig. 9.** Radiogenic isotopes for the Shaquanzi and Hongyuan intrusive rocks: (A) $\varepsilon_{Nd}(t)$ vs. $^{87}Sr/^{86}Sr(t)$ diagram ($t = 307.2$ Ma for the Shaquanzi gabbro and $t = 301.2$ Ma for the Hongyuan granodiorite), (B) $\varepsilon_{Nd}(t)$ vs. $^{206}Pb/^{204}Pb$ diagram after Zindler and Hart (1986), (C) $^{207}Pb/^{204}Pb$ vs. $^{206}Pb/^{204}Pb$ diagram and (D) $^{208}Pb/^{204}Pb$ vs. $^{206}Pb/^{204}Pb$ diagram after Li et al. (2001). Data for the Late Carboniferous CTT mafic–intermediate rocks are from Zhang et al. (2016a). NHRL = Northern Hemisphere reference line (Hart, 1984); BSE = bulk silicate earth, UC = upper crust, DM = depleted mantle, MORB = mid-oceanic ridge basalts, EM I = enriched mantle with low $^{87}Sr/^{86}Sr$, EM II = enriched mantle with high $^{87}Sr/^{86}Sr$, HIMU = high U/Pb mantle component (Zindler and Hart, 1986).

granodiorite samples have $I_{Sr}$ ratios of 0.704769–0.706211, $\varepsilon_{Nd}(t)$ values of $+0.38 - +1.86$ and $T_{DM}$ ages of 1.11–0.97 Ga. The initial $^{206}Pb/^{204}Pb$, $^{207}Pb/^{204}Pb$, and $^{208}Pb/^{204}Pb$ ratios of these samples are 17.461–18.299, 15.541–15.581 and 37.456–38.129, respectively (Table A.5). The Pb isotope compositions of these samples are generally uniform and plot between the mantle and the upper crustal growth curves, or close to the mantle line in the Pb isotope diagrams (Fig. 9C, D; Li et al., 2001).

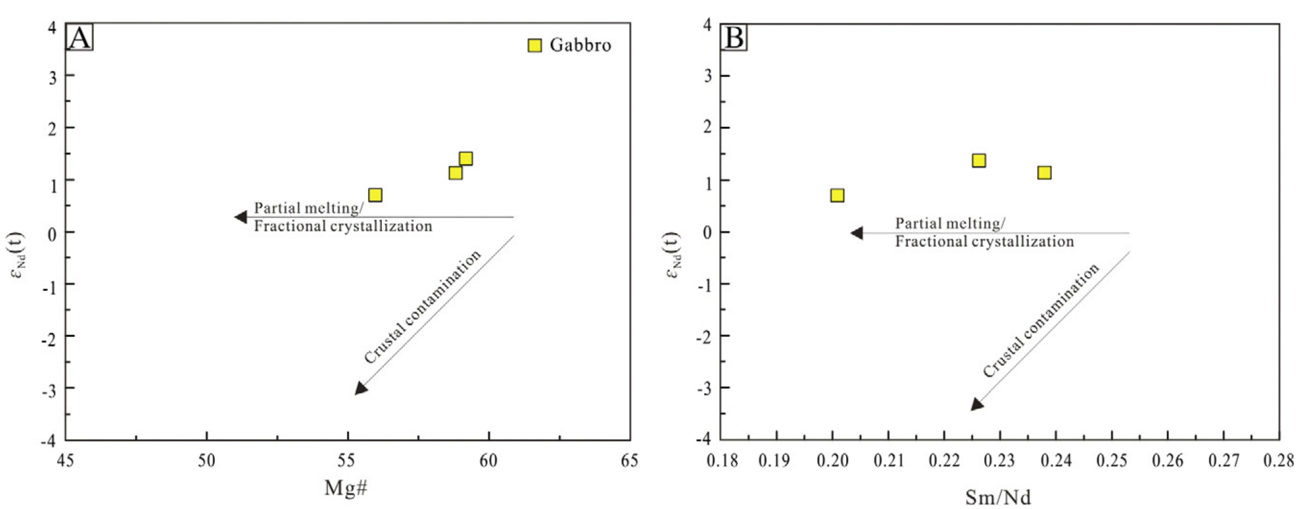


**Fig. 10.** (A) $\varepsilon_{Nd}(t)$ vs. Mg$^{\#}$ and (B) $\varepsilon_{Nd}(t)$ vs. Sm/Nd diagrams for the Shaquanzi gabbro.

## 5. Discussion

### 5.1. Petrogenesis and magma sources

Considering that rocks from the Shaquanzi and Hongyuan Pb–Zn deposits are partially altered, we focus largely on the immobile elements (e.g., Th, REEs and HFSEs) and transition elements (e.g., Sc, V, Ni and Cu) (Chen et al., 2013; Condie, 2005; Said and Kerrich, 2009; Winchester and Floyd, 1977) in our petrogenetic discussion.

#### 5.1.1. Shaquanzi gabbro

The Shaquanzi gabbro samples contain MgO of 5.2–6.3 wt%, with $Mg^{\#}$ values of 56–59, Ni of 7–24 ppm and Cr of 23–29 ppm, which are much lower than those of typical mantle-derived primary melts ($Mg^{\#} = 73–81$, Ni > 400 ppm and Cr > 1000 ppm; Wilson, 1989), indicating the presence of crystal fractionation. Fractionation of clinopyroxene and olivine is evidenced by the positive correlations between $Mg^{\#}$ values and Cr and Ni contents (Table A.1). Plagioclase fractionation is limited, as suggested by the lack of negative Sr and Eu anomalies (Fig. 6B). The distinct negative Nb, Ta and Ti anomalies of the gabbro rocks (Fig. 6B) may have been inherited from their sources that had been affected by crustal contamination or metasomatized by subduction-related fluids or Ti-minerals (such as rutile and spinel) fractionation (e.g., Hawkesworth et al., 1993; Lana et al., 2004; Saunders and Tamey, 1984).

Crustal contamination is common to the basaltic magmas that ascend through thick continental crust (Castillo et al., 1999; Watson, 1982). As shown in Fig. 6B, the Shaquanzi gabbro samples are enriched in LILEs (e.g., Rb, Ba, Pb) and depleted in HFSEs (e.g., Nb, Ta, Ti), which can be caused either by subduction or crustal contamination (Rudnick and Gao, 2003; Shinjo et al., 1999; Wang et al., 2013). Nevertheless, rocks formed by crustal contamination generally do not show distinct negative Zr–Hf anomalies because of the abundances of Zr and Hf in the crust (Qian et al., 2014). Because the Th/Nb ratio of basaltic magmas is independent of olivine, clinopyroxene and feldspar fractionation (Aldanmaz et al., 2000), mantle-derived mafic rocks tend to show diagnostic Th/Nb ratios, which can differentiate the relative input of crustal materials vs. subduction-related fluids (Li et al., 2013; Pearce, 2008). However, the absence of correlations between $Mg^{\#}$ and $\varepsilon_{Nd}(t)$ (Fig. 10A), or between $\varepsilon_{Nd}(t)$ and Sm/Nd (Fig. 10B), suggesting crustal contamination was not significant for the Shaquanzi gabbro samples. As shown in Fig. 11A, the gabbro samples have Th/Nb ratio of 0.23–1.00, plotting in the continental arc field, but far from the average upper continental crust (UCC). In addition, the gabbro samples have relatively high Ti/Zr (42.2–335.5) and Ti/Y (207.4–537.7) ratios, much higher than those (Ti/Zr < 30, Ti/Y < 200) of the typical crustal rocks (Wedepohl, 1995), precluding significant crustal contamination. This inference is further supported by the lack of correlations between the Sr–Nd isotopes and MgO (or $SiO_2$, Th/Nb, Ce/Nb) (Pearce and Cann, 1973; Sun and McDonough, 1989; Wood, 1980). As a strongly incompatible element, Th is enriched in sediments and the middle/upper crust (average middle and upper crust Th contents are ~6.5 and 10.5 ppm, respectively; Rudnick and Gao, 2003). However, thorium content is relatively low in the gabbro (average = 1.55 ppm), precluding significant involvement of crustal materials in the genesis of the gabbro samples.

Due to their similar crystal/melt partition coefficients, Nb and U are not significantly fractionated during crystallization (Hofmann, 1988; Sun and McDonough, 1989), and thus the Nb/U ratios can be used to identify mantle sources, e.g., oceanic basalts (Nb/U = ~50) (McDonough and Sun, 1995), continental crust (Nb/U = ~9) (Rudnick and Fountain, 1995) and arc volcanics (Nb/U = 0.3–9.0) (Chung et al., 2001). In the Nb vs. Nb/U diagram, three gabbro samples (Nb/U = 3.2–6.3) fall inside the arc volcanic field (Fig. 11B; Chung et al., 2001). In addition, the gabbro samples show selective enrichment of LILEs and LREEs and positive Sr anomalies in the primitive mantle-

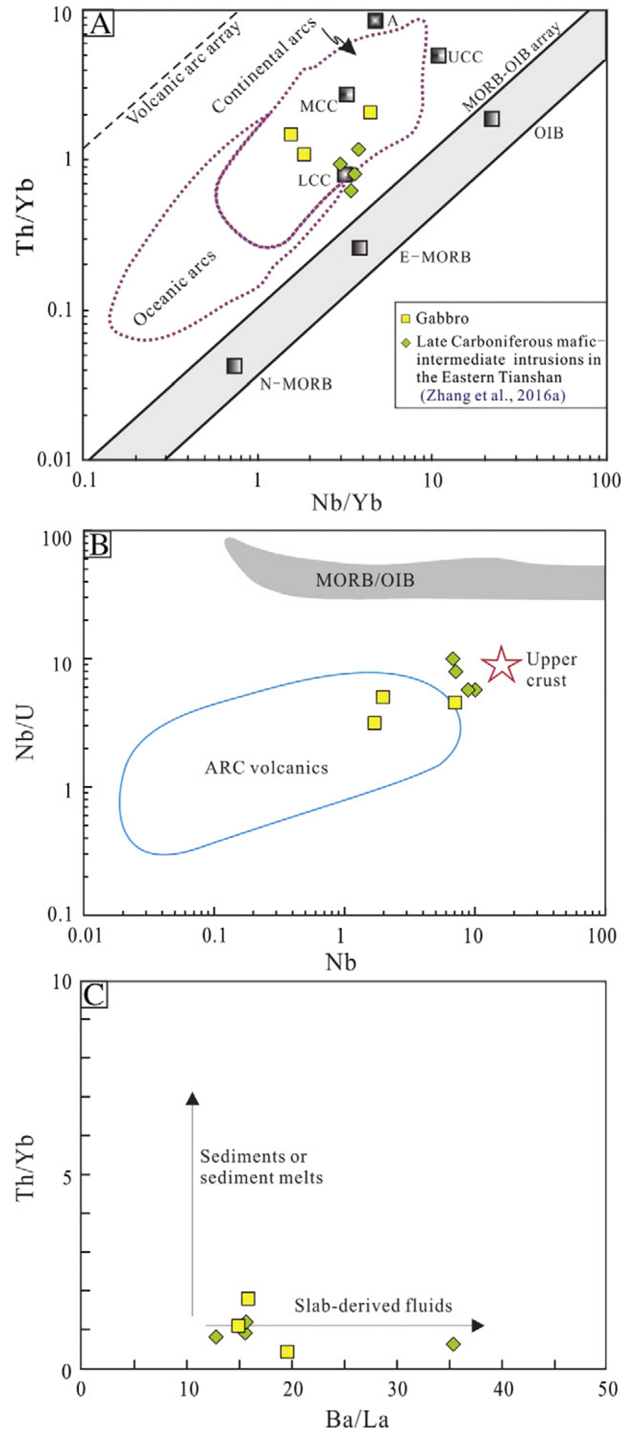


**Fig. 11.** (A) Th/Yb vs. Nb/Yb (Li et al., 2013; Pearce, 2008), (B) Nb/U vs. Nb (Chung et al., 2001) and (C) Th/Yb vs. Ba/La (Woodhead et al., 2001) diagrams for the CTT mafic–intermediate samples (Zhang et al., 2016a). Trace elements are plotted in ppm. Data source: MORB/OIB field are from McDonough and Sun (1995); the arc volcanic field is from Chung et al. (2001); Archaean (A) crust is from Rudnick and Fountain (1995); LCC, MCC and UCC are from Rudnick and Gao (2003).

normalized multi-element diagram (Fig. 6B), which suggests that their magma sources may have been metasomatized before the partial melting (Wang et al., 2013). Hydrous melts and slab-derived fluids are generally considered to be the two major metasomatic sources in subduction zones. Hydrous melts are capable to transport both water-soluble and water-insoluble materials, whereas slab-derived fluids are generally more capable to transport water-soluble materials (Zheng,

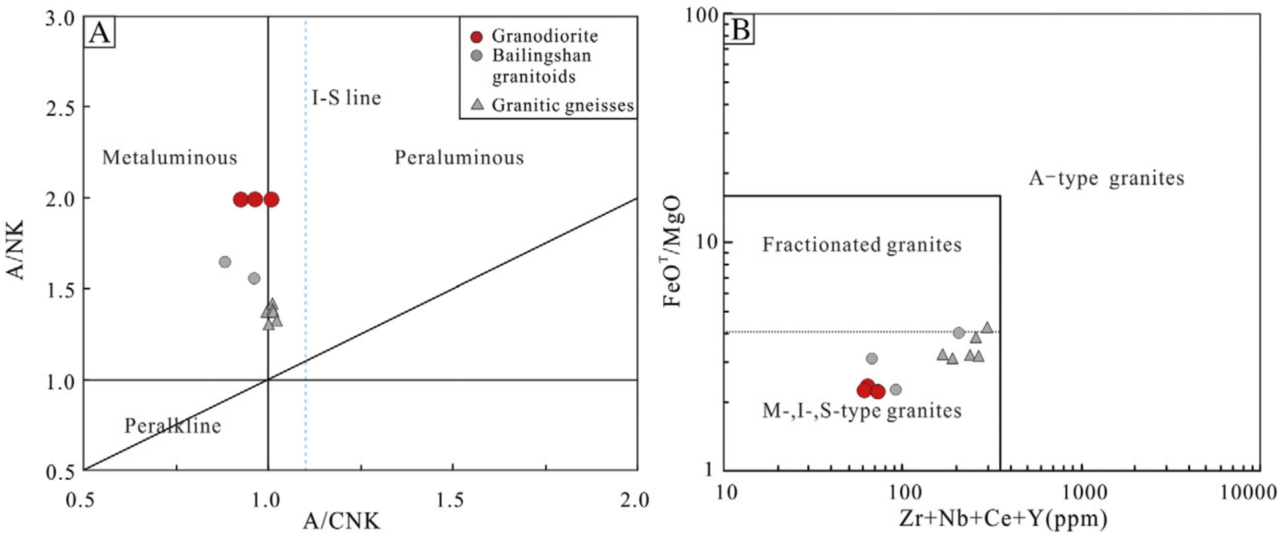


**Fig. 12.** (A) A/NK vs. A/CNK diagram (Maniar and Piccoli, 1989) and (B) FeO$^T$/MgO vs. (Zr + Nb + Ce + Y) diagram (Whalen et al., 1987). Data of the Late Carboniferous granites from CTT and Bailingshan are from Zhang et al. (2015b) and W.F. Zhang et al. (2016). A/CNK = molar $Al_2O_3$ / ($Na_2O$ + $K_2O$ + CaO), A/NK = molar $Al_2O_3$/($Na_2O$ + $K_2O$).

2012). In subduction zones, Ba/La fractionation can only be reasonably achieved by element mobility in hydrous fluids, while Th and LREEs are less mobile in slab-derived fluids but more mobile in melts (cf. HREEs and LILEs) (Woodhead et al., 2001). Therefore, element ratios such as Ba/La and Th/HREE are useful tracers of sediment inputs or fluid contributions (Woodhead et al., 2001). Our gabbro samples are characterized by variable Ba/La but uniform Th/Yb (Fig. 11C), indicating that the mantle sources may have been previously enriched by slab-derived fluids.

Geochemical signatures of the Shaquanzi gabbro, e.g., low $TiO_2$ (0.6–1.2 wt%) and enriched Sr–Nd isotopes argue against an asthenospheric mantle source, which generally produce magmatic rocks with high $TiO_2$ (average $TiO_2$ in OIB: 2.86 wt%) and depleted Sr–Nd isotopes (Han et al., 2015; Lightfoot et al., 1993; Wu et al., 2014). Thus, we suggest that the gabbro was probably derived from the sub-continental lithospheric mantle (SCLM) metasomatized by subduction-related fluids.

*5.1.2. Hongyuan granodiorite*

According to different magma sources, granites are genetically divided into M-, I-, S- and A-types (Chappell, 1999; Chappell and White, 1974; Frost et al., 2001). The Hongyuan granodiorite samples belong to medium-K calc-alkaline series (Fig. 5), which is geochemically comparable to the Late Carboniferous alkali-rich granitoids in the Eastern Tianshan (W.F. Zhang et al., 2016; Zhang et al., 2015b). The Hongyuan granodiorite is metaluminous (A/CNK = 0.93 to 1.01) (Fig. 12A; Table A.1), and can be classified as I-type according to Chappell and White (1974). In the (Zr + Nb + Ce + Y) vs. FeO$^T$/MgO diagram (Fig. 12B), the Hongyuan granodiorite and most Early Permian CTT granitoids fall in the M-, I-, S-type granites field (Chappell and White, 1992). Moreover, S-type granites contain Al-rich biotite and other Al-rich minerals, whereas I-type granites contain mainly hornblende; S-type granites commonly contain ilmenite rather than magnetite, whereas I-type granites contain mainly magnetite, although ilmenite-bearing varieties are also present (Chappell, 1999). Petrographic analysis shows that the Hongyuan granodiorite contains hornblende (Fig. 4D), but lack cordierite, garnet, monazite or ilmenite, suggesting that the samples are most likely I-type. Furthermore, the relatively low $I_{Sr}$ ratios of the Hongyuan granodiorite (0.704769–0.706211 < 0.707) also suggest an I-type origin (Chappell and White, 2001; Han and Ma, 2003).

Calc-alkaline I-type granitoids can be generated via (1) partial melting of mafic to intermediate (meta-) igneous rocks without sediment involvement (Chappell and White, 2001) or by (2) mixing of juvenile crustal-derived and mantle-derived magmas (Kemp et al., 2007). The Hongyuan granodiorite samples have Nb/Ta ratios of 12.6–12.9 and low contents of Ni, Cr and Co, indicating a crustal source (Green, 1995). Recent studies indicate that Hf isotopic compositions in zircons are useful in determining possible magma sources (e.g., Kemp et al., 2007; Woodhead et al., 2001; Wu et al., 2006). The Hongyuan granodiorite samples yielded $\varepsilon_{Hf}(t)$ values ranging from −10.26 to +5.57 (average of 1.34; Table A.4), suggesting that the magmas may have derived from a more juvenile source with contributions of older crustal sources (Kemp et al., 2007). In addition, the positive $\varepsilon_{Nd}(t)$ (+0.38 − +1.86) values (Table A.5) of the Hongyuan granodiorite also show juvenile source characteristics. Meanwhile, the Hongyuan granodiorite samples have relatively high Mg$^{\#}$ (52), implying the involvement of mantle-derived magmas. The initial $^{206}Pb/^{204}Pb$, $^{207}Pb/^{204}Pb$, and $^{208}Pb/^{204}Pb$ ratios of the Hongyuan granodiorite samples are 17.461–18.299, 15.541–15.581 and 37.456–38.129, respectively (Table A.5), plotting between the upper crust and the mantle, generally interpreted as a mixing between a fairly homogenized mantle- and upper crust reservoir (Fig. 9C, D). In conclusion, mingling of juvenile crust-derived magmas and mantle-derived magmas can account for the formation of the Hongyuan granodiorite.

*5.2. Tectonic and metallogenic implications*

*5.2.1. Tectonic implications for the Latest Carboniferous Eastern Tianshan*

Ophiolites in the northwestern Tianshan (Bayingou: ca. 325 Ma) (Dong et al., 2006; Xu et al., 2006) and West Junggar (Dabalar and Dalabuter: 531–332 Ma) (Jian et al., 2005) have been interpreted to represent remnants of the Junggar Ocean, which was a southern branch of the Paleo-Asian Ocean. The presence of ca. 325–320 Ma arc-related granitic gneiss (Zhang et al., 2015b) and ca. 312 Ma gabbros (Tang et al., 2012) in the northern margin of the CTT and ca. 317–307 Ma I-type Bailingshan granitoids (W.F. Zhang et al., 2016), 317–306 Ma Heijianshan-Chilongfeng intermediate–felsic rocks (Zhao et al., 2017) in the Aqishan-Yamansu Belt could be attributed to the south-dipping subduction of the Junggar oceanic plate. The Late Carboniferous (ca. 307 Ma) Shaquanzi gabbro is calc-alkaline and enriched in LILEs (e.g., K, Rb, Ba) and depleted in HFSEs (e.g., Nb, Ta, Ti) (Fig. 6), displaying typical subduction-related arc geochemical signatures and mostly plotting into the arc-related fields in the Hf/3–Th–Ta (Wood, 1980), Zr vs. $TiO_2$ (Pearce, 1982), and Zr vs. Ti (Pearce, 1996) discrimination diagrams (Fig. 13). These features may indicate a Late Carboniferous continental arc system along the northern margin of the CTT, formed by the southward subduction of the Junggar oceanic plate.

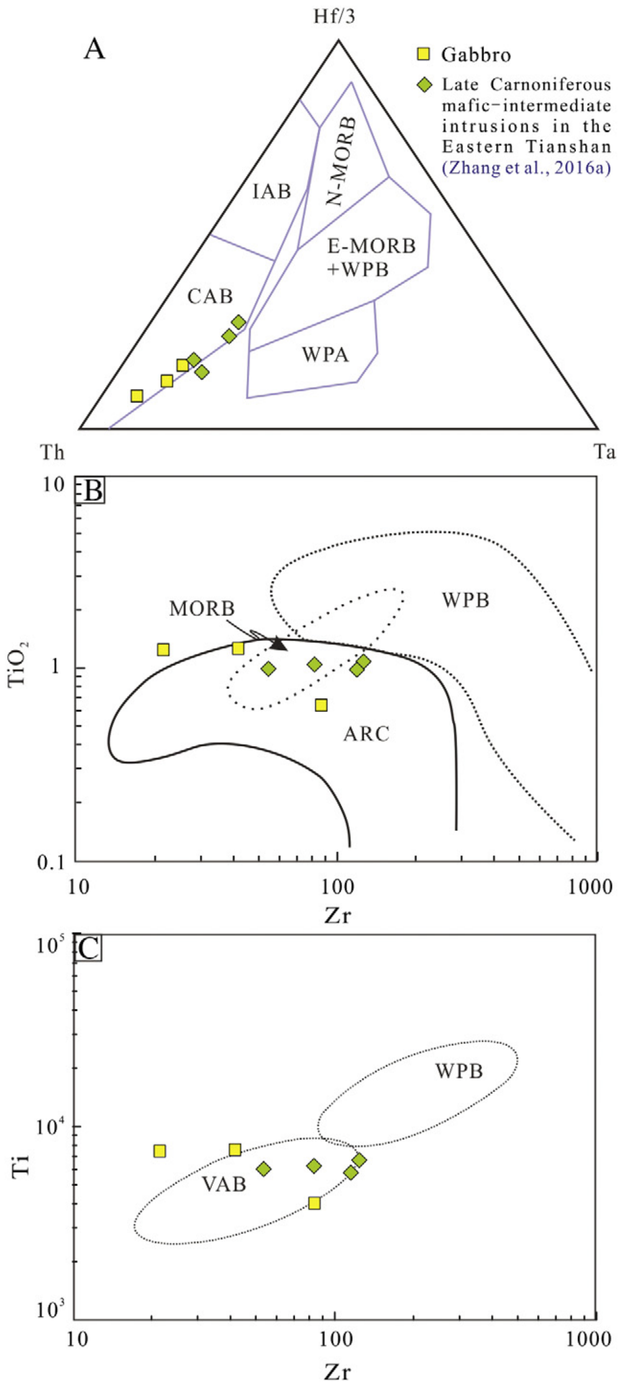


**Fig. 13.** Tectonic discrimination diagrams for the Shaquanzi gabbro. (A) Hf/3–Th–Ta diagram (Wood, 1980), (B) $TiO_2$ vs. Zr diagram (Pearce, 1982) and (C) Ti vs. Zr diagram (Pearce, 1996). Data for the Late Carboniferous CTT mafic–intermediate rocks are from Zhang et al. (2016a). CAB = continental arc calc-alkaline basalt, E-MORB = enriched mid-ocean ridge basalt, IAB = island arc calc-alkaline basalt, N-MORB = normal MORB, OIB = ocean island basalt, VAB = volcanic arc basalt, WPA = within plate alkaline basalt, WPB = within plate basalt, WPT = within plate tholeiites.

The Latest Carboniferous Hongyuan granodiorite (ca. 301 Ma), characterized by positive $\varepsilon_{Nd}(t)$ values (+0.38 − +1.86), low $I_{Sr}$ ratios (0.704769–0.706211) and high $Mg^{\#}$ (average of 52), mostly show VAG (volcanic arc granite) affinities in the widely-used trace element discrimination diagrams (Pearce et al., 1984; Fig. 14). Additionally, the Hongyuan granodiorite samples also show some syn-collisional affinities in the Nb vs. Y and Rb/10-Hf-Ta*3 diagrams (Fig. 14C, D; Harris et al., 1986; Pearce et al., 1984). Furthermore, some workers proposed that the 300 Ma shear zone-hosted Au deposits in the Kangguer shear zone were formed in syn-collisional stage (Han et al., 2010; Xiao et al., 2004). Consequently, we consider the ages of Shaquanzi gabbro and Hongyuan Granodiorite may have suggested a tectonic evolution from oceanic subduction to syn-collisional environment during the period of ca. 307–301 Ma in the Eastern Tianshan.

Moreover, previous studies indicate that the collisional regime in the Chinese Tianshan was ceased by the latest Carboniferous to Early Permian (Charvet et al., 2007; Chen et al., 2011; Zhang et al., 2015a, 2015b, 2016a). In addition, voluminous post-collisional magmatic rocks in the CTT were formed in the Early Permian, including ultramafic-mafic intrusions, mafic dyke swarms, granites and bimodal volcanic rocks (Chen et al., 2011; Han et al., 2004; Li et al., 2006; Ma et al., 2015). Zircons from mafic–ultramafic complexes in the Kangguer shear zone are mainly ~300–270 Ma during post-collisional stage and related to magmatic Cu–Ni sulfide mineralization (Mao et al., 2008; Qin et al., 2011; Su et al., 2013; Tang et al., 2011; Wang et al., 2006). The above evidence indicate the final closure of the Junggar Ocean and the subsequent collision and post-collision events between the CTT and Junggar block, occurring at ca. 300 Ma (Zhang et al., 2015b, 2016a, 2016c).

### *5.2.2. Implication for Pb–Zn mineralization*

Regionally, most of the Eastern Tianshan Pb–Zn deposits (e.g., Caixiashan, Hongyuan, Hongxingshan, Jiyuan, Shaquanzi and Yuxi) are hosted in the CTT Precambrian basement rocks. The metals were suggested to have precipitated through a variety of processes, including SEDEX-type (e.g., sedimentary stages of Caixiashan and Hongyuan; e.g. Cao et al., 2013; Gao et al., 2007; Li et al., 2016; Lu et al., 2017; Peng et al., 2006, 2007), sedimentation-hydrothermal reworking (Hongxingshan, Shaquanzi, Yuxi and skarn period of Hongyuan; e.g. Lu et al., 2017; Q.H. Xiao et al., 2009; Zhong et al., 2008; Zhou et al., 1999), and contact metasomatism (Jiyuan; e.g.H.Y. Chen et al., 2012).

Skarn alteration in Jiyuan is extensively developed along the intrusive contact between the Early Carboniferous diorite–granodiorite and the Precambrian marble, and occurred before the main Cu–Ag (–Zn) mineralization stage (H.Y. Chen et al., 2012). The giant Caixiashan Pb–Zn deposit had been modified by the Carboniferous magmatism (ca. 323 Ma; Gao et al., 2007; Cao et al., 2013; Peng et al., 2006, 2007). The Hongxingshan Pb–Zn and Yuxi Ag (–Pb–Zn) deposits have genetic relationships with the Late Carboniferous magmatism (Q.H. Xiao et al., 2009; Zhou et al., 1999). The Shaquanzi Pb–Zn deposit supports a genetic link between Shaquanzi gabbro (307 Ma) and the Pb–Zn mineralization (Zhong et al., 2008). Lu et al. (2017) indicated that the Hongyuan Pb–Zn mineralization may have firstly formed by Mesoproterozoic SEDEX-type processes, and then reworked and upgraded by the Late Carboniferous contact metasomatism during the granodiorite emplacement (ca. 301 Ma).

Regional geochemical characteristics indicate that the abundance of ore-forming elements (e.g. Pb, Zn, Ag) in the Precambrian basement is relatively high, suggesting high fertility in forming Pb–Zn deposits (Peng et al., 2006; Q.H. Xiao et al., 2009; Zhou et al., 1999). During the Early to Latest Carboniferous, S-dipping subduction beneath the CTT may have generated the continental arc magmatism (ca. 353–301 Ma) along the northern margin of the CTT. The associated hydrothermal alteration may have indirect links with the Pb–Zn mineralization (e.g., reworked/upgraded), forming a major Carboniferous Pb–Zn mineralization belt.

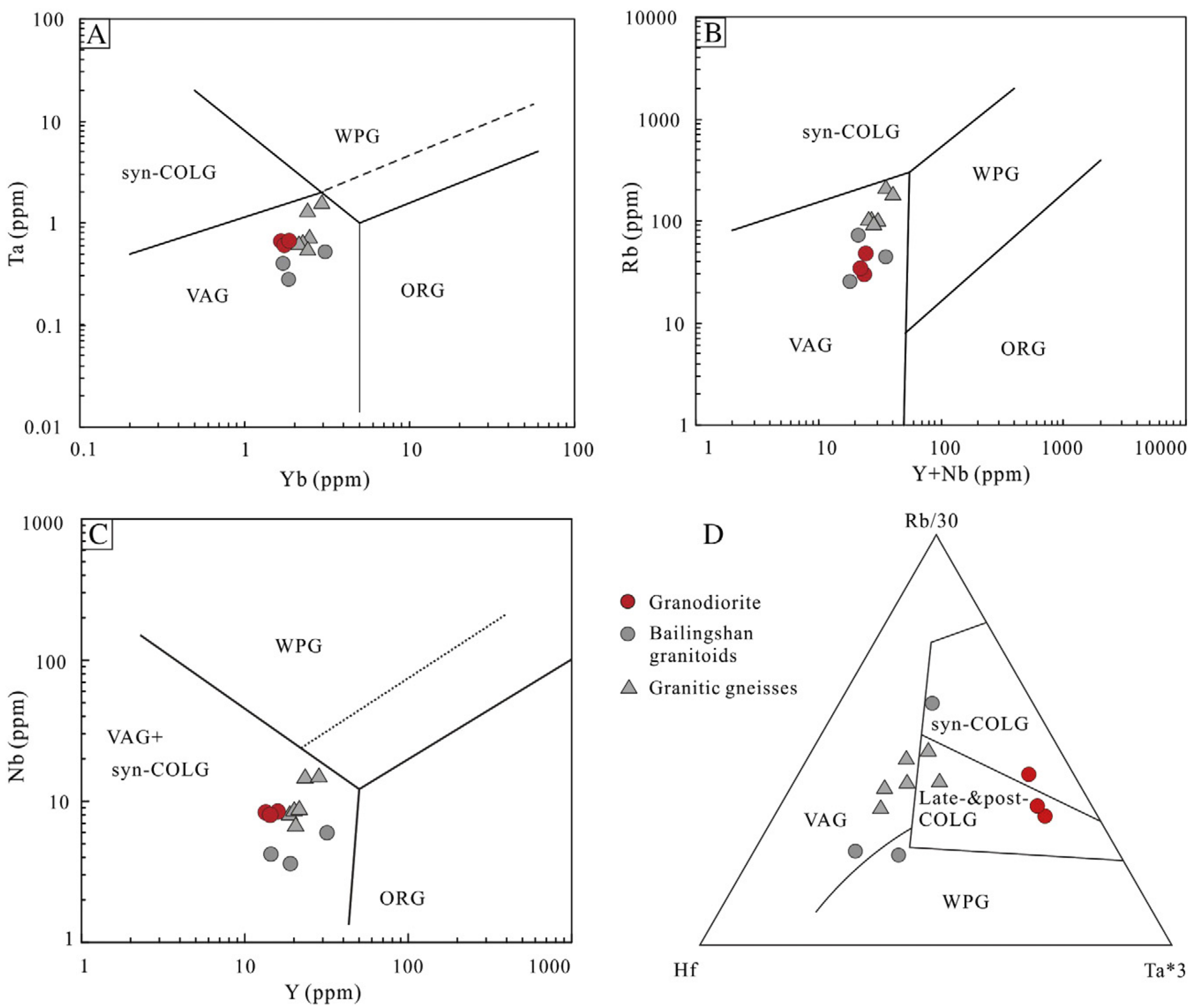


**Fig. 14.** Tectonic discrimination diagrams for the Hongyuan granodiorite. (A) Ta vs. Yb, (B) Rb vs. Y + Nb and (C) Nb vs. Y diagrams are from Pearce et al. (1984) with (D) Rb/30 − Hf − Ta*3 ternary diagram from Harris et al. (1986). ORG = Ocean Ridge Granite; WPG = Within Plate Granite; VAG = Volcanic Arc Granite; syn-COLG = syn-Collisional Granite.

## 6. Conclusions

(1) LA-ICP-MS zircon U–Pb dating of the Shaquanzi gabbro and the Hongyuan granodiorite yielded Late Carboniferous ages of 307.2 ± 1.5 Ma and 301.2 ± 1.5 Ma, respectively.

(2) Petrological and geochemical data indicate that primary magma of the Shaquanzi gabbro samples may have been derived from the SCLM metasomatized by subduction-related fluids,whereas the Hongyuan I-type granodiorite were likely to be derived from partial melting of juvenile crust sources mixed with some mantle-derived materials.

(3) Combined our geochemical study of the Shaquanzi gabbro and Hongyuan granodiorite with previous investigations, we suggest a tectonic evolution from oceanic subduction to syn-collisional extension during the period of ca. 307–301 Ma in the Eastern Tianshan.

(4) Most of the Eastern Tianshan Pb–Zn deposits had indirect (reworked/upgraded) links with the Carboniferous magmatism.

Supplementary data to this article can be found online at https://doi.org/10.1016/j.lithos.2017.10.009.

## Acknowledgements

We appreciate the editor (Sun-Lin Chung) and two reviewers' (Wenjiao Xiao and Xiaoran Zhang) for their constructive suggestions and comments to improve the manuscript. We are also grateful to Congying Li, Le Zhang, Jinlong Ma (Guangzhou Institute of Geochemistry, CAS) for their help during zircon and whole-rock analyses, and Pei Liang, Chao Wu and Chao Xu (Guangzhou Institute of Geochemistry, CAS) for their help in the manuscript preparation, and the staffs from the Xinjiang Bureau of Geology and Mineral Resources (BGMR) for their field support. This study was funded by Chinese National Basic Research 973-Program (2014CB440802), the Strategic Priority Research Program (B) of Chinese Academy of Sciences (CAS) (XDB1803206), CAS Creative and Interdisciplinary Program (Y433131A07), CAS–SAFEA International Partnership Program for Creative Research Teams (20140491534).

## References

Aldanmaz, E., Pearce, J.A., Thirlwall, M.F., Mitchell, J.G., 2000. Petrogenetic evolution of late Cenozoic, post-collision volcanism in western Anatolia, Turkey. Journal of Volcanology and Geothermal Research 102, 67–95.

Allen, M.B., Windley, B.F., Zhang, C., 1993. Paleozoic collisional tectonics and magmatism of the Chinese Tien Shan, central Asia. Tectonophysics 220, 89–115.

Cao, X.F., Lü, X.B., Zhang, P., Liu, S.T., Gao, X., Liu, Y.G., Tang, R.K., Wang, Y.J., Hu, Q.T., 2013. Stable isotope geochemistry and ore genesis of the Caixiashan Pb–Zn deposit in eastern Middle Tianshan, Xinjiang. Journal of Central South University (Science and Technology) 44, 662–672 (in Chinese with English abstract).
Castillo, P.R., Janney, P.E., Solidum, R.U., 1999. Petrology and geochemistry of Camiguin Island, southern Philippines: insights to the source of adakites and other lavas in a complex arc setting. Contributions to Mineralogy and Petrology 134, 33–51.
Chappell, B.W., 1999. Aluminum saturation in I- and S-type granites and the characterization of fractionated haplogranites. Lithos 46, 535–551.
Chappell, B.W., White, A.J.R., 1974. Two contrasting granite types. Pacific Geology 8, 173–174.
Chappell, B.W., White, A.J.R., 1992. I- and S-type granites in the Lachlan Fold Belt. Geological Society of America Special Papers 272, 1–26.
Chappell, B.W., White, A.J.R., 2001. Two contrasting granite types: 25 years later. Australian Journal of Earth Sciences 48, 489–499.
Charvet, J., Shu, L., Laurent-Charvet, S., 2007. Paleozoic structural and geodynamic evolution of eastern Tianshan (NW China): welding of the Tarim and Junggar plates. Episodes 30, 162–186.
Chen, X.J., Shu, L.S., Santosh, M., 2011. Late Paleozoic post-collisional magmatism in the Eastern Tianshan Belt, Northwest China: new insights from geochemistry, geochronology and petrology of bimodal volcanic rocks. Lithos 127, 581–598.
Chen, Y.J., Pirajno, F., Wu, G., Qi, J.P., Xiong, X.L., 2012a. Epithermal deposits in north Xinjiang, NW China. International Journal of Earth Sciences 101, 889–917.
Chen, H.Y., Yang, J.T., Baker, M., 2012b. Mineralization and fluid evolution of the Jiyuan polymetallic Cu–Ag–Pb–Zn–Au deposit, eastern Tianshan, NW China. International Geology Review 54, 816–832.
Chen, X.J., Shu, L.S., Santosh, M., Zhao, X.X., 2013. Island arc-type bimodal magmatism in the eastern Tianshan Belt, Northwest China: geochemistry, zircon U–Pb geochronology and implications for the Paleozoic crustal evolution in Central Asia. Lithos 168, 48–66.
Chung, S.L., Wang, K.L., Crawford, A.J., Kamenetsky, V.S., Chen, C.H., Lan, C.Y., Chen, C.H., 2001. High-Mg potassic rocks from Taiwan: implications for the genesis of orogenic potassic lavas. Lithos 59, 153–170.
Condie, K.C., 2005. High field strength element ratios in Archean basalts: a window to evolving sources of mantle plumes? Lithos 79, 491–504.
Deng, X.H., Wang, J.B., Wang, Y.W., Li, Y.C., Fang, T.H., Mao, Q.G., 2014. Geological characteristics of the Hongshi Cu–Au deposit, eastern Tianshan, Xinjiang and discussion of the deposit genesis. Mineral Exploration 5, 159–168 (in Chinese with English abstract).
Dong, Y.P., Zhou, D.W., Zhang, G.W., Zhao, X., Luo, J.H., Xu, J.G., 2006. Geology and geochemistry of the Gangou ophiolitic mélange at the northern margin of the Middle Tianshan Belt. Acta Petrologica Sinica 22, 49–56 (in Chinese with English abstract).
Frost, B.R., Barnes, C.G., Collins, W.J., Arculus, R.J., Ellis, D.J., Frost, C.D., 2001. A geochemical classification for granitic rocks. Journal of Petrology 42, 2033–2048.
Gao, J., Klemd, R., 2003. Formation of HP-LT rocks and their tectonic implications in the western Tianshan Orogen, NW China: geochemical and age constraints. Lithos 66, 1–22.
Gao, Z.J., Chen, J.Z., Lu, S.N., 1993. Precambrian System of the Northern Xinjiang. Geological Publishing House, Beijing, pp. 1–153 (in Chinese).
Gao, J., Li, M.S., Xiao, X.C., Tang, Y.Q., He, G.Q., 1998. Paleozoic tectonic evolution of the Tianshan Orogen, northwestern China. Tectonophysics 287, 213–231.
Gao, J.G., Peng, M.X., Liang, T., Wang, L., Wang, D.H., Li, Y.L., 2007. Research on the geology and isotopic geochemistry of the Caixiashan Pb–Zn deposit in Xinjiang. Journal of Earth Sciences and Environment 29, 137–140 (in Chinese with English abstract).
Gao, J., Long, L.L., Klemd, R., Qian, Q., Liu, D.Y., Xiong, X.M., Su, W., Liu, W., Wang, Y.T., Yang, F.Q., 2009. Tectonic evolution of the South Tianshan orogen and adjacent regions, NW China: geochemical and age constraints of granitoid rocks. International Journal of Earth Sciences 98, 1221–1238.
Green, T.H., 1995. Significance of Nb/Ta as an indicator of geochemical processes in the crust-mantle system. Chemical Geology 120, 347–359.
Han, J.W., Ma, Z.D., 2003. Isotope Geochemistry. In: Ma, Z.D., Zhang, H.F. (Eds.), Geochemistry Special Publication. 225. Geology Publishing House, Beijing, pp. 213–266 (in Chinese).
Han, B.F., Ji, J.Q., Song, B., Chen, L.H., Li, Z.G., 2004. SHRIMP zircon U–Pb dating of the Kalatongke and Huangshandong mafic-ultramafic complex-bearing Cu–Ni ores, Xinjiang, and geological implications. Science Bulletin of China 49, 2324–2328 (in Chinese).
Han, B.F., Guo, Z.J., Zhang, Z.C., Zhang, L., Chen, J.F., Song, B., 2010. Age, geochemistry, and tectonic implications of a late Paleozoic stitching pluton in the North Tian Shan suture zone, western China. Geological Society of America Bulletin 122, 627–640.
Han, J.S., Chen, H.Y., Yao, J.M., Deng, X.H., 2015. 2.24 Ga mafic dykes from Taihua Complex, southern Trans-North China Orogen, and their tectonic implications. Precambrian Research 270, 124–138.
Harris, N.B.W., Pearce, J.A., Tindle, A.G., 1986. Geochemical characteristics of collision-zone magmatism. Geological Society, London, Special Publications 19, 67–81.
Hart, S.R., 1984. A large-scale isotope anomaly in the Southern Hemisphere mantle. Nature 309, 753–757.
Hawkesworth, C.J., Gallagher, K., Hergt, J.M., McDermott, F., 1993. Mantle and slab contribution in arc magmas. Annual Review of Earth and Planetary Sciences 21, 175–204.
He, Z.Y., Zhang, Z.M., Zong, K.Q., Xiang, H., Chen, X.J., Xia, M.J., 2014. Zircon U–Pb and Hf isotopic studies of the Xingxingxia Complex from Eastern Tianshan (NW China): significance to the reconstruction and tectonics of the southern Central Asian Orogenic Belt. Lithos 190–191, 485–499.
Hofmann, A.W., 1988. Chemical differentiation of the Earth: the relationship between mantle, continental crust, and oceanic crust. Earth and Planetary Science Letters 90, 297–314.
Hoskin, P.W.O., Schaltegger, U., 2003. The composition of zircon and igneous and metamorphic petrogenesis. Reviews in Mineralogy and Geochemistry 53, 27–62.
Hu, A.Q., Zhang, Z.G., Liu, J.Y., Peng, J.H., Zhang, J.B., Zhao, D.J., Yang, S.Z., Zhou, W., 1986. U–Pb age and evolution of Precambrian metamorphic rocks of middle Tianshan uplift zone, eastern Tianshan, China. Geochimica 23–35 (in Chinese with English abstract), 1.
Hu, A.Q., Jahn, B.M., Zhang, G.X., Chen, Y.B., Zhang, Q.F., 2000. Crustal evolution and Phanerozoic crustal growth in northern Xinjiang: Nd isotopic evidence. Part I. Isotopic characterization of basement rocks. Tectonophysics 328, 15–51.
Huang, B.T., He, Z.Y., Zhang, Z.M., Klemd, R., Zong, K.Q., Zhao, Z.D., 2015. Early Neoproterozoic granitic gneisses in the Chinese Eastern Tianshan: petrogenesis and tectonic implications. Journal of Asian Earth Sciences 113, 339–352.
Jahn, B.M., Wu, F., Chen, B., 2000. Massive granitoid generation in Central Asia: Nd isotope evidence and implication for continental growth in the Phanerozoic. Episodes 23, 82–92.
Jian, P., Liu, D.Y., Shi, Y.R., Zhang, F.Q., 2005. SHRIMP Dating of SSZ Ophiolites from Northern Xinjiang Province, China: Implications for Generation of Oceanic Crust in the Central Asian Orogenic Belt. In: Sklyarov, E.V. (Ed.), Structural and Tectonic Correlation Across the Central Asia Orogenic Collage: North-Eastern Segment; Guide-book and Abstract Volume of the Siberian Workshop IGCP-480. Institute of the Earth Crust, Siberian Branch of Russian Academy of Sciences, Irkutsk, pp. 1–246.
Kemp, A.I.S., Hawkesworth, C.J., Foster, G.L., Paterson, B.A., Woodhead, J.D., Hergt, J.M., Gray, C.M., Whitehouse, M.J., 2007. Magmatic and crustal differentiation history of granitic rocks from hafnium and oxygen isotopes in zircon. Science 315, 980–983.
Lana, C., Reimold, W.U., Gibson, R.L., Koeberl, C., Siegesmund, S., 2004. Nature of the Archean midcrust in the core of the Vredefort Dome, Central Kaapvaal Craton, South Africa. Geochimica et Cosmochimica Acta 68, 623–642.
Laurent-Charvet, S., Charvet, J., Shu, L.S., Ma, R., Lu, H.F., 2002. Paleozoic late collisional strike-slip deformations in Tianshan and Altay, Eastern Xinjiang, NW China. Terra Nova 14, 249–256.
Lei, R.X., Wu, C.Z., Gu, L.X., Zhang, Z.Z., Chi, G.X., Jiang, Y.H., 2011. Zircon U–Pb chronology and Hf isotope of the Xingxingxia granodiorite from the Central Tianshan zone (NW China): implications for the tectonic evolution of the southern Altaids. Gondwana Research 20, 582–593.
Li, L., Zheng, Y.F., Zhou, J.B., 2001. Dynamic model for Pb isotope evolution in the continental crust of China. Acta Petrologica Sinica 17, 61–68 (in Chinese with English abstract).
Li, J.Y., Song, B., Wang, K.Z., Li, Y.P., Sun, G.H., Qi, D.Y., 2006. Permian mafic–ultramafic complexes on the southern margin of the Tu–Ha basin, East Tianshan Mountains: geological records of vertical crustal growth in Central Asia. Acta Geoscientica Sinica 27, 424–446 (in Chinese with English abstract).
Li, Q.G., Liu, S.W., Wang, Z.Q., Yan, Q.R., Guo, Z.J., Zhang, Z.C., Zheng, H.F., Jiang, C.F., Wang, T., Chu, Z.Y., 2007. Geochemical constraints on the petrogenesis of the Proterozoic granitoid gneisses from the eastern segment of the Central Tianshan Tectonic Zone, northwestern China. Geological Magazine 144, 305–317.
Li, B., Bagas, L., Gallardo, L.A., Said, N., Diwu, C., McCuaig, T.C., 2013. Back-arc and post-collisional volcanism in the Paleoproterozoic Granites-Tanami Orogen, Australia. Precambrian Research 224, 570–587.
Li, D.F., Zhang, L., Chen, H.Y., Hollings, P., Cao, M.J., Fang, J., Wang, C.M., Lu, W.J., 2016. Geochronology and geochemistry of the high Mg dioritic dikes in Eastern Tianshan, NW China: geochemical features, petrogenesis and tectonic implications. Journal of Asian Earth Sciences 115, 442–454.
Lightfoot, P.C., Hawkesworth, C.J., Hergt, J., Naldrett, A.J., Gorbachev, N.S., Fedorenko, V.A., Doherty, W., 1993. Remobilization of the continental lithosphere by a mantle plume: major-, trace-element, and Sr-, Nd-, Pb-isotope evidence from picritic and tholeiitic lavas of the Noril'sk District, Siberian Trap, Russia. Contrib. Mineralogy and Petrology 114, 171–188.
Liu, S.W., Guo, Z.J., Zhang, Z.C., Li, Q.G., Zheng, H.F., 2004. Nature of the Precambrian metamorphic blocks in the eastern segment of Central Tianshan: constraint from geochronology and Nd isotopic geochemistry. Science in China Series D: Earth Sciences 47, 1085–1094.
Long, L.L., Gao, J., Xiong, X.M., Qian, Q., 2006. The geochemical characteristics and the age of the Kule Lake ophiolite in the southern Tianshan. Acta Petrologica Sinica 22, 65–73 (in Chinese with English abstract).
Lu, W.J., Zhang, L., Chen, H.Y., Han, J.S., Jiang, H.J., Li, D.F., Fang, J., Wang, C.M., Zheng, Y., Tan, Z.X., 2017. Geology, fluid inclusion and isotope geochemistry of the Hongyuan reworked sediment-hosted Zn–Pb deposit: Metallogenic implications for Zn–Pb deposits in the Eastern Tianshan, NW China. Ore Geology Reviews. https://doi.org/10.1016/j.oregeorev.2017.01.004.
Luo, F.Z., 1989. On Precambrian of Central Tianshan uplift (metamorphic) zone. Xinjiang Geology 7, 24–33 (in Chinese).
Ma, R.S., Shu, L.S., Sun, J.Q., 1997. Tectonic Evolution and Metallogeny of Eastern Tianshan Mountains. Geological Publishing House.
Ma, X.X., Shu, L.S., Meert, J.G., Li, J.Y., 2014. The Paleozoic evolution of Central Tianshan: geochemical and geochronological evidence. Gondwana Research 25, 797–819.
Ma, X.X., Shu, L.S., Meert, J.G., 2015. Early Permian slab break off in the Chinese Tianshan belt inferred from the post-collisional granitoids. Gondwana Research 27, 228–243.
Maniar, P.D., Piccoli, P.M., 1989. Tectonic discrimination of granitoids. Geological Society of America Bulletin 101, 635–643.
Mao, J.W., Pirajno, F., Zhang, Z.H., Chai, F.M., Wu, H., Chen, S.P., Cheng, S.L., Yang, J.M., Zhang, C.Q., 2008. A review of the Cu–Ni sulfide deposits in the Chinese Tianshan and Altay orogens (Xinjiang Autonomous Region, NW China): principal characteristics and ore-forming processes. Journal of Asian Earth Sciences 32, 184–203.

McDonough, W.F., Sun, S.S., 1995. The composition of the Earth. Chemical Geology 120, 223–253.

Müller, D., Rock, N.M.S., Groves, D.I., 1992. Geochemical discrimination between shoshonitic and potassic volcanic rocks in different tectonic settings: a pilot study. Mineralogy and Petrology 46, 259–289.

Pearce, J.A., 1982. Trace Element Characteristics of Lavas from Destructive Plate Boundaries. In: Thorpe, R.S. (Ed.), Orogenic Andesites and Related Rocks. John Wiley and Sons, Chichester, England, pp. 528–548.

Pearce, J.A., 1996. Sources and settings of granitic rocks. Episodes 19, 120–125.

Pearce, J.A., 2008. Geochemical fingerprinting of oceanic basalts with applications to ophiolite classification and the search for Archean oceanic crust. Lithos 100, 14–48.

Pearce, J.A., Cann, J.R., 1973. Tectonic setting of basic volcanic rocks determined using trace element analyses. Earth and Planetary Science Letters 19, 290–300.

Pearce, J.A., Harris, N.B.W., Tindle, A.G., 1984. Trace element discrimination diagrams for the tectonic interpretation of granitic rocks. Journal of Petrology 25, 956–983.

Peccerillo, A., Taylor, S.R., 1976. Geochemistry of Eocene calc-alkaline volcanic rocks from the Kastamonu area, northern Turkey. Contrib. Mineralogy and Petrology 58, 63–81.

Peng, M.X., Wang, J.L., Yu, W.Y., Zhang, Z., Zhang, T., Wang, W.J., 2006. Geological characteristics features and building about prospecting model of the Caixia Hill lead–zinc deposit in the Shanshan, Xinjiang. Xinjiang Geology 24, 405–411 (in Chinese with English abstract).

Peng, M.X., Sang, S.J., Zhu, C., Chen, J., Wu, L.B., Liang, T., Wu, X.J., Wu, H.P., 2007. Forming analysis of the Caixia lead–zinc deposit, Xinjiang and comparison with the MVT deposit forming. Xinjiang Geology 25, 373–378 (in Chinese with English abstract).

Qian, Y., Ge, W.C., Yang, H., Zhao, G.C., Zhang, Y.L., Su, L., 2014. Petrogenesis of late Paleozoic volcanic rocks from the Daheshen Formation in central Jilin Province, NE China, and its tectonic implications: constraints from geochronology, geochemistry and Sr-Nd-Hf isotopes. Lithos 192, 116–131.

Qin, K.Z., Su, B.S., Sakyi, P.A., Tang, D.M., Li, X.H., Sun, H., Xiao, Q.H., Liu, P.P., 2011. SIMS zircon U–Pb geochronology and Sr–Nd isotopes of Ni-Cu-bearing mafic-ultramafic intrusions in Eastern Tianshan and Beishan in correlation with flood basalts in Tarim Basin (NW China): constraints on a ca. 280 Ma mantle plume. American Journal of Science 311, 237–260.

Rubatto, D., 2002. Zircon trace element geochemistry: partitioning with garnet and the link between U–Pb ages and metamorphism. Chemical Geology 184, 123–138.

Rudnick, R.L., Fountain, D.M., 1995. Nature and composition of the continental crust: a lower crustal perspective. Reviews of Geophysics-Richmond Virginia then Washington 33, 267–309.

Rudnick, R.L., Gao, S., 2003. Composition of the continental crust. Treatise on Geochemistry 3, 1–64.

Said, N., Kerrich, R., 2009. Geochemistry of coexisting depleted and enriched Paringa Basalts, in the 2.7 Ga Kalgoorlie Terrane, Yilgarn Craton, Western Australia: evidence for a heterogeneous mantle plume event. Precambrian Research 174, 287–309.

Saunders, A.D., Tamey, J., 1984. Geochemical Characteristics of Basaltic Volcanism within Back-arc Basins. In: Kokelaar, B.P., Howells, M.F. (Eds.), Marginal Basin Geology: Geological Society of Special Publication, London. vol. 16, pp. 59–76.

Sengör, A.M.C., Natal'in, B.A., 1996. Paleotectonics of Asia: Fragments of Synthesis. In: Yin, A., Harrison, T.M. (Eds.), The Tectonic Evolution of Asia. Cambridge University Press, Cambridge, pp. 480–640.

Sengör, A.M.C., Natal'in, B.A., Burtman, V.S., 1993. Evolution of the Altaid tectonic collage and Paleozoic crustal growth in Eurasia. Nature 364, 299–307.

Shi, Y.R., Jian, P., Kroner, A., Jahn, B.M., Liu, D.Y., Zhang, W., Ma, H.D., 2014. Zircon ages and Hf isotopic compositions of plutonic rocks from the Central Tianshan (Xinjiang, northwest China) and their significance for early to mid-Paleozoic crustal evolution. International Geology Review 56, 1413–1434.

Shinjo, R., Chung, S.L., Kato, Y., Kimura, M., 1999. Geochemical and Sr-Nd isotopic characteristics of volcanic rocks from the Okinawa Trough and Ryukyu arc: implications for the evolution of a young, intracontinental back arc basin. Journal of Geophysical Research - Solid Earth 104, 10591–10608.

Shu, L.S., Charvet, J., Guo, L.Z., Lu, H.F., Laurent-Charvet, S., 1999. A large-scale Paleozoic dextral ductile strike-slip zone: the Aqqikkudug–Weiya Zone along the Northern margin of the Central Tianshan Belt, Xinjiang, NW China. Acta Geologica Sinica 73, 148–162.

Shu, L.S., Yu, J.H., Charvet, J., Laurent-Charvet, S., Sang, H.Q., Zhang, R.G., 2004. Geological, geochronological and geochemical features of granulites in the Eastern Tianshan, NW China. Journal of Asian Earth Sciences 24, 25–41.

Su, B.X., Qin, K.Z., Tang, D.M., Sakyi, P.A., Liu, P.P., Sun, H., Xiao, Q.H., 2013. Late Paleozoic mafic–ultramafic intrusions in southern Central Asian Orogenic Belt (NW China): insight into magmatic Ni–Cu sulfide mineralization in orogenic setting. Ore Geology Reviews 51, 57–73.

Sun, S.S., McDonough, W.F., 1989. Chemical and Isotopic Systematics of Oceanic Basalts: Implications for Mantle Composition and Processes. In: Saunders, A.D., Norry, M.J. (Eds.), Magmatism in the Ocean Basins. Geological Society, London, Special Publications 42, pp. 313–345.

Tang, D.M., Qin, K.Z., Li, C.S., Qi, L.S., Su, B.X., Qu, W.J., 2011. Zircon dating, Hf–Sr–Nd–Os isotopes and PGE geochemistry of the Tianyu sulfide-bearing mafic–ultramafic intrusion in the Central Asian Orogenic Belt, NW China. Lithos 126, 84–98.

Tang, G.J., Wang, Q., Wyman, D.A., Li, Z.X., Zhao, Z.H., Yang, Y.H., 2012. Late Carboniferous high $\varepsilon_{Nd}(t)$–$\varepsilon_{Hf}(t)$ granitoids, enclaves and dikes in western Junggar, NW China: ridge-subduction-related magmatism and crustal growth. Lithos 140–141, 86–102.

Wang, J.B., Wang, Y.W., He, Z.J., 2006. Ore deposits as a guide to the tectonic evolution in the East Tianshan Mountains, NW China. Geology in China 33, 461–469 (in Chinese with English abstract).

Wang, B., Shu, L.S., Faure, M., Jahn, B.M., Cluzel, D., Charvet, J., Chung, S.L., Meffre, S., 2011. Paleozoic tectonics of the southern Chinese Tianshan: insights from structural, chronological and geochemical studies of the Heiyingshan ophiolitic mélange (NW China). Tectonophysics 497, 85–104.

Wang, H., Wu, Y.B., Qin, Z.W., Zhu, L.Q., Liu, Q., Liu, X.C., Gao, S., Wijbrans, J.R., Zhou, L., Gong, H.J., 2013. Age and geochemistry of Silurian gabbroic rocks in the Tongbai orogen, central China: implications for the geodynamic evolution of the North Qinling arc-back-arc system. Lithos 179, 1–15.

Watson, E.B., 1982. Basalt contamination by continental crust: some experiments and models. Contributions to Mineralogy and Petrology 80, 73–87.

Wedepohl, K.H., 1995. The composition of the continental crust. Geochimica et Cosmochimica Acta 59, 1217–1232.

Whalen, J.B., Currie, K.L., Chappell, B.W., 1987. A-type granites: geochemical characteristics, discrimination and petrogenesis. Contributions to Mineralogy and Petrology 95, 407–419.

Wilson, M., 1989. Igneous Petrogenesis-A Global Tectonic Approach. Unwin Hyman, London, p. 466.

Winchester, J.A., Floyd, P.A., 1977. Geochemical discrimination of different magma series and their differentiation products using immobile elements. Chemical Geology 20, 325–343.

Windley, B.F., Allen, M.B., Zhang, C., Zhao, Z.Y., Wang, G.R., 1990. Paleozoic accretion and cenozoic redeformation of the Chinese Tien-Shan-Range, Central-Asia. Geology 18, 128–131.

Windley, B.F., Alexeiev, D., Xiao, W., Kröner, A., Badarch, G., 2007. Tectonic models for accretion of the Central Asian Orogenic belt. Journal of the Geological Society of London 164, 31–47.

Wood, D.A., 1980. The application of a Th–Hf–Ta diagram to problems of tectonomagmatic classification and to establishing the nature of crustal contamination of basaltic lavas of the British tertiary volcanic province. Earth and Planetary Science Letters 50, 11–30.

Woodhead, J.D., Hergt, J.M., Davidson, J.P., Eggins, S.M., 2001. Hafnium isotope evidence for 'conservative' element mobility during subduction zone process. Earth and Planetary Science Letters 192, 331–346.

Wu, F.Y., Yang, Y.H., Xie, L.W., Yang, J.H., Xu, P., 2006. Hf isotopic compositions of the standard zircons and baddeleyites used in U–Pb geochronology. Chemical Geology 234, 105–126.

Wu, C.Z., Santosh, M., Chen, Y.J., Samson, I.M., Lei, R.X., Dong, L.H., Qu, X., Gu, L.X., 2014. Geochronology and geochemistry of Early Mesoproterozoic meta-diabase sills from Quruqtagh in the northeastern Tarim Craton: implications for breakup of the Columbia supercontinent. Precambrian Research 241, 29–43.

Xiao, W.J., Zhang, L.C., Qin, K.Z., Sun, S., Li, J.L., 2004. Paleozoic accretionary and collisional tectonics of the Eastern Tianshan (China): implications for the continental growth of central Asia. American Journal of Science 304, 370–395.

Xiao, W.J., Han, C.M., Yuan, C., Sun, M., Lin, S., Chen, H.L., Li, Z.L., Li, J.L., Sun, S., 2008. Middle Cambrian to Permian subduction–related accretionary orogenesis of Northern Xinjiang, NW China: implications for the tectonic evolution of central Asia. Journal of Asian Earth Sciences 32, 102–117.

Xiao, W.J., Windley, B.F., Huang, B.C., Han, C.M., Yuan, C., Chen, H.L., Sun, M., Sun, S., Li, J.L., 2009a. End-Permian to mid-Triassic termination of the accretionary processes of the southern Altaids: implications for the geodynamic evolution, Phanerozoic continental growth, and metallogeny of Central Asia. International Journal of Earth Sciences 98, 1189–1217.

Xiao, Q.H., Qin, K.Z., Xu, Y.X., San, J.Z., Ma, Z.L., Sun, H., Tang, D.M., 2009b. A discussion on geological characteristics of Hongxingshan Pb–Zn (Ag) deposit in Middle Tianshan massif, eastern Xinjiang, with reference to regional metallogenesis. Mineral Deposits 120–132 (in Chinese with English abstract).

Xiao, W.J., Li, S.Z., Santosh, M., Jahn, B.M., 2012. Orogenic belts in Central Asia: correlations and connections. Journal of Asian Earth Sciences 49, 1–6.

Xiao, W.J., Windley, B.F., Sun, S., Li, J.L., Huang, B.C., Han, C.M., Yuan, C., Sun, M., Chen, H.L., 2015. A tale of amalgamation of three collage systems in the permianmiddle Triassic in Central-East Asia: oroclines, sutures, and terminal accretion. Annual Review of Earth and Planetary Sciences 43, 477–507.

Xiu, Q.Y., Yu, H.F., Li, Q., 2002. A single zircon U–Pb age for the granodiorite of Kawabulark Complex, Xinjiang, China. Xinjiang Geology 20, 335–337 (in Chinese with English abstract).

Xu, X.Y., Xia, L.Q., Ma, Z.P., Wang, Y.B., Xia, Z.C., Li, X.M., Wang, L.S., 2006. SHRIMP zircon U–Pb geochronology of the plagiogranites from Bayingou ophiolite in North Tianshan Mountains and the petrogenesis of the ophiolite. Acta Petrologica Sinica 22, 83–94 (in Chinese with English abstract).

Zhang, Z.Z., Gu, L.X., Wu, C.Z.L.W.Q., Xi, A.H., Wang, S., 2005. Zircon SHRIMP dating for the Weiya pluton, Eastern Tianshan: its geological implications. Acta Geologica Sinica (English Edition) 79, 481–490.

Zhang, X.R., Zhao, G.C., Eizenhöfer, P.R., Sun, M., Han, Y.G., Hou, W.Z., Liu, D.X., Wang, B., Liu, Q., Xu, B., 2015a. Paleozoic magmatism and metamorphism in the Central Tianshan Block revealed by U–Pb and Lu–Hf isotope studies of detrital zircons from the South Tianshan belt, NW China. Lithos 233, 193–208.

Zhang, X.R., Zhao, G.C., Eizenhöfer, P.R., Sun, M., Han, Y.G., Hou, W.Z., Liu, D.X., Wang, B., Liu, Q., Xu, B., 2015b. Latest Carboniferous closure of the Junggar Ocean constrained by geochemical and zircon U–Pb–Hf isotopic data of granitic gneisses from the Central Tianshan Block, NW China. Lithos 238, 26–36.

Zhang, W.F., Chen, H.Y., Han, J.S., Zhao, L.D., Huang, J.H., Yang, J.T., Yan, X.L., 2016a. Geochronology and geochemistry of igneous rocks in the Bailingshan area: implications for the tectonic setting of late Paleozoic magmatism and iron skarn mineralization in the eastern Tianshan, NW China. Gondwana Research 38, 40–59.

Zhang, X.R., Zhao, G.C., Eizenhöfer, P.R., Sun, M., Han, Y.G., Hou, W.Z., Liu, B.W., Liu, Q., Xu, B., Zhu, C.Y.L., 2016b. Tectonic transition from Late Carboniferous subduction to Early Permian post-collisional extension in the Eastern Tianshan, NW China: insights from geochronology and geochemistry of mafic-intermediate intrusions. Lithos 256, 269–281.

Zhang, X.R., Zhao, G.C., Eizenhöfer, P.R., Sun, M., Han, Y.G., Hou, W.Z., Liu, D.X., Wang, B., Liu, Q., Xu, B., 2016c. Late Ordovician adakitic rocks in the Central Tianshan block, NW China: partial melting of lower continental arc crust during back-arc basin opening. Geological Society of America Bulletin 128, 1367–1382.

Zhang, X.R., Zhao, G.C., Sun, M., Eizenhöfer, P.R., Han, Y.G., Hou, W.Z., Liu, D.X., Wang, B., Liu, Q., Xu, B., 2016d. Tectonic evolution from subduction to arc-continent collision of the Junggar ocean: constraints from U-Pb dating and Hf isotopes of detrital zircons from the North Tianshan belt, NW China. Geological Society of America Bulletin 128, 644–660.

Zhang, X.R., Zhao, G.C., Eizenhöfer, P.R., Sun, M., Han, Y.G., Hou, W.Z., Liu, D.X., Wang, B., Liu, Q., Xu, B., 2017. Varying contents of sources affect tectonic setting discrimination of sediments: a case study from Permian sandstones in the Eastern Tianshan, northwestern China. The Journal of Geology. https://doi.org/10.1086/691217.

Zhao, L.D., Chen, H.Y., Zhang, L., Zhang, W.F., Yang, J.T., Yan, X.L., 2017. The Late Paleozoic magmatic evolution of the Aqishan-Yamansu belt, Eastern Tianshan: constraints from geochronology, geochemistry and Sr–Nd–Pb–Hf isotopes of igneous rocks. Journal of Asian Earth Sciences. https://doi.org/10.1016/j.jseaes.2017.07.038.

Zheng, Y.F., 2012. Metamorphic chemical geodynamics in continental subduction zones. Chemical Geology 328, 5–48.

Zhong, F.S., Cheng, S.L., Wang, R.J., Hao, G.L., Deng, G., 2008. The characteristics and genesis of the Shaquanzi Pb–Zn deposit. Xinjiang Nonferrous Metals 31, 11–14 (in Chinese).

Zhou, J.Y., Cui, B.F., Lu, Y., 1999. Characteristics and genesis of the Yuxi deposit in Hami, Xinjiang. Mineral Deposits 18, 209–218 (in Chinese with abstract).

Zhou, T.F., Yuan, F., Zhang, D.Y., Fan, Y., Liu, S., Peng, M.X., Zhang, J.D., 2010. Geochronology, tectonic setting and mineralization of granitoids in Jueluotage area, eastern Tianshan, Xingjiang. Acta Petrologica Sinica 26, 478–502 (in Chinese with English abstract).

Zindler, A., Hart, S., 1986. Chemical geodynamics. Annual Review of Earth and Planetary Sciences 14, 493–571.